Risk and Return Spillovers among the G10 Currencies

Matthew Greenwood-Nimmo[a], Viet Hoang Nguyen[b], Barry Rafferty[a,*]

[a]*Department of Economics, University of Melbourne, 111 Barry Street, Melbourne 3053, Australia.*
[b]*Melbourne Institute of Applied Economic & Social Research, 111 Barry Street, Melbourne 3053, Australia.*

Abstract

We study spillovers among daily returns and innovations in option-implied risk-neutral volatility and skewness of the G10 currencies. An empirical network model uncovers substantial time variation in the interaction of risk measures and returns, both within and between currencies. We find aggregate spillover intensity is countercyclical with respect to the federal funds rate and increases in periods of financial stress. During these times, volatility spillovers and especially skewness spillovers between currencies increase, reflecting greater systematic risk. Also during these times, we find greater linkages between returns and risk measures, as returns become more sensitive to risk measures and vice versa.

Keywords: Foreign exchange markets, risk-neutral volatility, risk-neutral skewness, spillovers, coordinated crash risk.

JEL Classifications: C58, F31, G01, G15.

*Corresponding author. Tel.: +61 (0)3-8344-7198.

Email addresses: matthew.greenwood@unimelb.edu.au (Matthew Greenwood-Nimmo), vietn@unimelb.edu.au (Viet Hoang Nguyen), barry.rafferty@unimelb.edu.au (Barry Rafferty)

1. Introduction

It is well established that investors may reduce their exposure to idiosyncratic risk by holding diversified portfolios. Consequently, investors in the foreign exchange (FX) markets form and manage portfolios conditional on the risk-return profiles of a set of currencies. Characterising these risk-return profiles is, however, challenging because currency investors face a variety of risks. The FX asset pricing literature emphasises both the volatility and the skewness of changes in the exchange rate as key components of a currency's risk profile.

Volatility has long been used as a measure of uncertainty and a sophisticated literature has documented the linkage between returns and volatility. For example, Menkhoff, Sarno, Schmeling, and Schrimpf (2012) show that differences in exposure to innovations in an aggregate measure of global FX volatility play an important role in explaining the cross-sectional differences in the average excess returns of interest rate sorted currency portfolios and, therefore, in the average excess returns to the carry trade strategy. Changes in global FX volatility have also been shown to help to predict carry trade returns in the time series dimension by Bakshi and Panayotov (2013).

Skewness, meanwhile, measures 'crash risk', the risk associated with large jumps or crashes in the exchange rate, whether depreciations or appreciations. Crash risk has gained considerable attention as a factor underlying the high average excess returns to various currency strategies. A negative cross-sectional relationship between interest rate differentials and currency skewness has been documented at the individual currency level by Brunnermeier, Nagel, and Pedersen (2009) and Jurek (2014). Furthermore, Rafferty (2012) demonstrates that exposure to a global FX skewness measure explains a large proportion of the high average excess returns not just to the carry trade but also to currency momentum and value strategies. Rafferty's global FX skewness measure captures the risk of a *coordinated crash*, in which high yield investment currencies sharply depreciate and low yield funding currencies simultaneously appreciate. Coordinated crashes were observed during the global financial crisis (GFC), as funding liquidity constraints led to the the sudden unwinding of carry trades.[1]

[1] Another significant branch of the crash risk literature considers the importance of crash risk by comparing the returns to carry trades hedged using options versus unhedged carry trades (Burnside, Eichenbaum, Kleshchelski, and Rebelo, 2011; Jurek, 2014; Farhi, Fraiberger, Gabaix, Rancier, and Verdelhan, 2014). The results strongly suggest that a significant proportion of the average excess returns to the carry trade can be attributed to crash risk.

A key message arising from this literature is that changes in currencies' volatility and skewness profiles will be reflected in their returns. This, in turn, has implications for portfolio rebalancing by currency investors. As investors buy and sell currencies to achieve their desired rebalancing, their actions may induce further changes in the currencies' risk-return profiles. This endogeneity creates a feedback effect which will be manifested in a complex array of interactions — or spillovers — among currency returns, volatility and skewness, both within individual currency markets and between currency markets. Network analysis provides a natural framework within which to study such complex dynamic interactions. Network models have recently risen to prominence in several areas of applied finance (Diebold and Yilmaz, 2009, 2014; Billio, Getmansky, Lo, and Pelizzon, 2012), yet they remain largely absent from the FX literature. We therefore develop an empirical network model to study spillovers of risk and return within and between currency markets.

Given the importance of portfolio rebalancing in the network dynamics of the FX markets, our model has two salient features. First, in recognition of the fact that FX portfolios are typically composed of several currencies, we work with a comprehensive panel dataset covering the G10 currencies. These ten currencies are among the world's most actively traded and liquid, collectively accounting for the large majority of turnover in global FX markets according to statistics published by the Bank for International Settlements[2]. By achieving good cross-sectional coverage of the FX markets, we are therefore able to capture the large majority of investors' rebalancing activities.

Second, given that portfolio rebalancing is generally forward-looking, our analysis is based on forward-looking measures of volatility and skewness extracted from options data. Option-implied measures of volatility and skewness confer several advantages as risk measures (Christoffersen, Jacobs, and Chang, 2013; Chang, Christoffersen, and Jacobs, 2013; Conrad, Dittmar, and Ghysels, 2013). Since they are computed every day using one day of options prices, they provide truly conditional market-based estimates of the risk-neutral expected volatility and skewness that investors anticipate over the option maturity. As such, in contrast with latent and realised measures of volatility and skewness, the option-implied measures capture investors' beliefs and risk preferences in a forward-looking manner which reflects ex ante measures of expected volatility and skewness.

[2]The Bank for International Settlements publishes a triennial survey of turnover in foreign exchange markets, the most recent of which is available at http://www.bis.org/publ/rpfx13fx.pdf.

To recover the moments of the option-implied (risk-neutral) distribution of future exchange rate changes, we use the model-free methodology of Bakshi and Madan (2000), Carr and Madan (2001) and Bakshi, Kapadia, and Madan (2003).[3] In this way, we construct daily option-implied measures of volatility and skewness for each of the G10 currencies against the U.S. dollar over the period January 1999 to October 2014 using a rich dataset of FX options prices obtained from J.P. Morgan. To account for the autocorrelation structure of the risk-neutral moments, we follow the precedent established by Menkhoff et al. (2012) and Chang et al. (2013) in the equity literature and extract the innovations in the risk-neutral volatility (RNV) and skewness (RNS) of exchange rate changes based on auxiliary first order autoregressions.

We construct our network model using a generalisation of the connectedness framework developed by Diebold and Yilmaz (2009, 2014), in which one infers the structure of a network based on forecast error variance decomposition of an underlying vector autoregressive model. The generalisation that we employ is due to Greenwood-Nimmo, Nguyen, and Shin (2015a), whose method accommodates arbitrary aggregations of the connectedness matrix. The benefit of this approach is that it provides a means to transform the connectedness matrix to directly capture connectedness among groups of variables (e.g. among currency markets, where we observe the return, RNV and RNS innovations for each market) as opposed to connectedness among individual variables.

Our analysis proceeds in two parts. First, we establish a benchmark by evaluating the connectedness among currencies over the full sample period, from January 1999 to October 2014. This reveals significant spillovers among returns, with particularly strong bilateral spillovers among currencies that share an underlying linkage, including the European currencies and also the commodity currencies. Similarly, spillovers of RNV innovations across currencies exert a strong influence over the evolution of volatility, accounting for as much as 75% of the ten-days-ahead forecast error variance of RNV innovations. By contrast, currency-specific or idiosyncratic factors tend to dominate the behaviour of RNS innovations, reflecting the importance of market-specific shocks in driving the risk of large jumps or crashes in exchange rates.

Next, we analyse time variation in the pattern and intensity of spillovers using 250-day rolling

[3] A sizeable literature has studied the role of option-implied volatility and skewness in asset pricing, particularly with respect to equity markets (Ang, Hodrick, Xing, and Zhang, 2006, 2009; Chang et al., 2013; Conrad et al., 2013). A growing literature has applied similar techniques to the FX markets (Chen and Gwati, 2014; Jurek, 2014).

samples. This reveals that aggregate spillover intensity is inversely related to the federal funds rate, indicating that spillovers strengthen (weaken) as economic and financial conditions in the U.S. deteriorate (improve). Similarly, spillovers intensify during periods of illiquidity (captured via the TED spread) and periods of uncertainty in equity markets (represented by the VIX). Adverse shocks — particularly the GFC and the European sovereign debt crisis — are associated with a marked increase in spillover activity. Spillovers from RNV and RNS innovations to realised returns pick up substantially during the crises, reflecting investors rebalancing their portfolios to manage their risk exposures. Interestingly, cross-market skewness spillovers intensify particularly markedly at this time, indicating a sharp increase in coordinated crash risk.

Our paper can be viewed as a logical development of the literature on volatility spillovers initiated by Engle, Ito, and Lin (1990). Most of the early papers in this literature use models in the GARCH family to construct latent measures of conditional volatility (e.g. Kearney and Patton, 2000; Hong, 2001). More recently, the focus has shifted toward the use of high-frequency realised volatility measures (e.g. Melvin and Melvin, 2003; Cai, Howorka, and Wongswan, 2008; Bubák, Kočenda, and Žikeš, 2011). We are aware of just one study which uses option-implied volatilities. Nikkinen, Sahlström, and Vähämaa (2006) work with option-implied volatilities derived from the Garman and Kohlhagen (1983) model to study volatility transmission in three currency pairs using just two years of data. None of these studies employ network models and none account for the interaction of returns with higher-order moments. Consequently, our work significantly extends the frontier demarcated by the existing literature.

This paper proceeds in 7 sections. Section 2 reviews the connectedness framework developed by Diebold and Yilmaz (2009, 2014) and shows how it can be extended to measure spillovers among groups of variables. Section 3 discusses the data sources and outlines the computation of the model-free option-implied risk-neutral moments of the distribution of expected exchange rate changes. Our estimation results are analysed in Sections 4–6, including a raft of robustness exercises. Section 7 concludes. Additional technical details are collected in three appendices.

2. Empirical Framework

We consider the bilateral exchange rates for $i = 1, 2, \ldots, N$ currencies, each quoted against the U.S. dollar and observed at daily frequency over $t = 1, 2, \ldots, T$ trading days. For each currency market, we observe the return, r_{it}, the innovation in risk-neutral volatility, v_{it} and the innovation in risk-neutral skewness, s_{it}. Detailed definitions of these three variables are provided in Section 3. The 3×1 vector $\boldsymbol{y}_{it} = (r_{it}, v_{it}, s_{it})'$ collects the market-specific variables for the i-th market and the $3N \times 1$ vector $\boldsymbol{y}_t = (\boldsymbol{y}'_{1t}, \boldsymbol{y}'_{2t}, \ldots, \boldsymbol{y}'_{Nt})'$ contains all of the variables for every market. The total number of variables in the system is $d = 3N$.

Abstracting from deterministic terms for clarity of exposition, the p-th order reduced form vector autoregression for the $d \times 1$ vector of all variables $\boldsymbol{y}_t$ may be written as follows:

$$\boldsymbol{y}_t = \sum_{j=1}^{p} \boldsymbol{A}_j \boldsymbol{y}_{t-j} + \boldsymbol{u}_t \tag{1}$$

where the $\boldsymbol{A}_j$'s are $d \times d$ matrices of unknown coefficients and $\boldsymbol{u}_t \sim N(\boldsymbol{0}, \boldsymbol{\Sigma}_u)$, where $\boldsymbol{\Sigma}_u$ is the symmetric positive definite covariance matrix of the reduced form residuals. The reduced form VAR model in (1) has the following infinite order moving average representation:

$$\boldsymbol{y}_t = \sum_{j=0}^{\infty} \boldsymbol{B}_j \boldsymbol{u}_{t-j} \tag{2}$$

where the $\boldsymbol{B}_j$'s are the moving average parameters which are square-summable and causal and are defined recursively as $\boldsymbol{B}_j = \boldsymbol{A}_1 \boldsymbol{B}_{j-1} + \boldsymbol{A}_2 \boldsymbol{B}_{j-2} + \ldots$ for $j = 1, 2, \ldots$ with $\boldsymbol{B}_0 = \boldsymbol{I}_d$ and $\boldsymbol{B}_j = \boldsymbol{0}$ for $j < 0$. Pesaran and Shin (1998) show that the h-step-ahead generalised forecast error variance decomposition (GVD) for the i-th variable is given by:

$$\vartheta_{i \leftarrow j}^{(h)} = \frac{\sigma_{u,jj}^{-1} \sum_{\ell=0}^{h-1} \left(\boldsymbol{\epsilon}_i' \boldsymbol{B}_\ell \boldsymbol{\Sigma}_u \boldsymbol{\epsilon}_j \right)^2}{\sum_{\ell=0}^{h-1} \boldsymbol{\epsilon}_i' \boldsymbol{B}_\ell \boldsymbol{\Sigma}_u \boldsymbol{B}_\ell' \boldsymbol{\epsilon}_i} \tag{3}$$

for $i, j = 1, \ldots, d$, where $\sigma_{u,jj}$ is the jth diagonal element of $\boldsymbol{\Sigma}_u$, $\boldsymbol{\epsilon}_i$ is a $d \times 1$ selection vector with its i-th element set to unity and zeros elsewhere. $\vartheta_{i \leftarrow j}^{(h)}$ expresses the proportion of the h-step-ahead forecast error variance (FEV) of variable i which can be attributed to shocks in the equation for variable j. Unlike orthogonalized forecast error variance decomposition which relies on Cholesky factor exact identification of the disturbance terms, GVDs are order invariant. However, because the computation of GVDs does not involve orthogonalization of the disturbances, it will generally

be the case that $\sum_{j=1}^{d} \vartheta_{i\leftarrow j}^{(h)} > 1$ due to the non-zero correlation between reduced form shocks. Following Diebold and Yilmaz (2014), the percentage interpretation of the FEV shares can be restored by normalising such that $\theta_{i\leftarrow j}^{(h)} = 100 \times \left(\vartheta_{i\leftarrow j}^{(h)} / \sum_{j=1}^{d} \vartheta_{i\leftarrow j}^{(h)}\right) \%$.

The key insight of Diebold and Yilmaz (2009, 2014) is that normalised GVDs can be used to construct a weighted directed network among the variables in a VAR system. The h-step-ahead $d \times d$ connectedness matrix among the d variables in $\boldsymbol{y}_t$ is given by:

$$\mathbb{C}^{(h)} = \begin{bmatrix} \theta_{1\leftarrow 1}^{(h)} & \theta_{1\leftarrow 2}^{(h)} & \cdots & \theta_{1\leftarrow d}^{(h)} \\ \theta_{2\leftarrow 1}^{(h)} & \theta_{2\leftarrow 2}^{(h)} & \cdots & \theta_{2\leftarrow d}^{(h)} \\ \vdots & \vdots & \ddots & \vdots \\ \theta_{d\leftarrow 1}^{(h)} & \theta_{d\leftarrow 2}^{(h)} & \cdots & \theta_{d\leftarrow d}^{(h)} \end{bmatrix} \tag{4}$$

The h-step-ahead FEV for variable i may be decomposed into the elements of the i^{th} *row* of $\mathbb{C}^{(h)}$. Following Diebold and Yilmaz (2009), we define the following quantities:

$$O_{i\leftarrow i}^{(h)} = \theta_{i\leftarrow i}^{(h)} \;\; ; \;\; F_{i\leftarrow j}^{(h)} = \theta_{i\leftarrow j}^{(h)} \;\; \text{and} \;\; F_{i\leftarrow \bullet}^{(h)} = \sum_{j=1, j\neq i}^{d} \theta_{i\leftarrow j}^{(h)} \; . \tag{5}$$

The proportion of the h-step-ahead FEV of the i-th variable that can be attributed to shocks to variable i itself is known as the *own variance share*, $O_{i\leftarrow i}^{(h)}$. The spillover to variable i from variable j is measured by $F_{i\leftarrow j}^{(h)}$, which records the proportion of variable i's h-step-ahead FEV attributable to shocks in variable j. Consequently, the total spillover from the system to variable i is given by $F_{i\leftarrow \bullet}^{(h)}$, which is referred to as the *from* connectedness of variable i.

The spillovers originating from the i-th variable can be characterised by:

$$T_{j\leftarrow i}^{(h)} = \theta_{j\leftarrow i}^{(h)} \;\; \text{and} \;\; T_{\bullet\leftarrow i}^{(h)} = \sum_{j=1, j\neq i}^{d} \theta_{j\leftarrow i}^{(h)} \; . \tag{6}$$

The spillover to variable j from variable i is captured by $T_{j\leftarrow i}^{(h)}$. Note that $\mathbb{C}^{(h)}$ will typically be asymmetric and so $\theta_{i\leftarrow j}^{(h)} \neq \theta_{j\leftarrow i}^{(h)}$ when $i \neq j$. Hence, the spillover measures derived from (4) are directional. The total spillover from variable i to the system is measured by $T_{\bullet\leftarrow i}^{(h)}$ and is referred to as the *to* connectedness of variable i. With these quantities in hand, it is straightforward to compute the *net* h-step-ahead connectedness of variable i as follows:

$$N_i^{(h)} = T_{\bullet\leftarrow i}^{(h)} - F_{i\leftarrow \bullet}^{(h)} \; . \tag{7}$$

Finally, the overall role of own-variable effects and spillovers in the system as a whole may be captured by the following two magnitudes, respectively:

$$H^{(h)} = \frac{1}{d}\sum_{i=1}^{d} O_{i\leftarrow i}^{(h)} \quad \text{and} \quad S^{(h)} = \frac{1}{d}\sum_{i=1}^{d} F_{i\leftarrow \bullet}^{(h)} = \frac{1}{d}\sum_{i=1}^{d} T_{\bullet\leftarrow i}^{(h)} \ . \tag{8}$$

where $H^{(h)}$ denotes the aggregate own-variable effect and $S^{(h)}$ is the aggregate *spillover index*. Note that $H^{(h)} + S^{(h)} = 100\%\ \forall h$.

The Diebold-Yilmaz framework can be used either to measure spillovers among individual variables or to summarise aggregate spillover activity among all variables in the system being studied. However, it does not provide a simple way to measure spillovers among *groups* of variables. As such, it is not straightforward to apply the Diebold-Yilmaz technique to measure spillovers among multiple markets, each of which is represented by the three variables: r_{it}, v_{it} and s_{it}. Consequently, Greenwood-Nimmo et al. (2015a) develop a generalised framework which exploits block aggregation of the connectedness matrix. Block aggregation introduces a new stratum between the level of individual variables and the systemwide aggregate level, thereby enhancing the flexibility of the Diebold-Yilmaz framework.

Suppose that the variables are in the order $\boldsymbol{y}_t = (r_{1t}, v_{1t}, s_{1t}, r_{2t}, v_{2t}, s_{2t}, \ldots, r_{Nt}, v_{Nt}, s_{Nt})'$ and that we wish to evaluate the connectedness among the N markets in the model in a combined manner that encompasses all three variables in each market. Following Greenwood-Nimmo et al. (2015a), we may write the connectedness matrix $\mathbb{C}^{(h)}$ in block form with $g = N$ groups each composed of $m = 3$ variables as follows:

$$\mathbb{C}^{(h)} = \begin{bmatrix} \mathbf{B}_{1\leftarrow 1}^{(h)} & \mathbf{B}_{1\leftarrow 2}^{(h)} & \cdots & \mathbf{B}_{1\leftarrow N}^{(h)} \\ \mathbf{B}_{2\leftarrow 1}^{(h)} & \mathbf{B}_{2\leftarrow 2}^{(h)} & \cdots & \mathbf{B}_{2\leftarrow N}^{(h)} \\ \vdots & \vdots & \ddots & \vdots \\ \mathbf{B}_{N\leftarrow 1}^{(h)} & \mathbf{B}_{N\leftarrow 2}^{(h)} & \cdots & \mathbf{B}_{N\leftarrow N}^{(h)} \end{bmatrix}, \quad \mathbf{B}_{i\leftarrow j}^{(h)} = \begin{bmatrix} \theta_{r_i\leftarrow r_j}^{(h)} & \theta_{r_i\leftarrow v_j}^{(h)} & \theta_{r_i\leftarrow s_j}^{(h)} \\ \theta_{v_i\leftarrow r_j}^{(h)} & \theta_{v_i\leftarrow v_j}^{(h)} & \theta_{v_i\leftarrow s_j}^{(h)} \\ \theta_{s_i\leftarrow r_j}^{(h)} & \theta_{s_i\leftarrow v_j}^{(h)} & \theta_{s_i\leftarrow s_j}^{(h)} \end{bmatrix} \tag{9}$$

for $i, j = 1, 2, \ldots, N$ and where the block $\mathbf{B}_{i\leftarrow i}^{(h)}$ collects all the within-market effects for market i while $\mathbf{B}_{i\leftarrow j}^{(h)}$ collects all spillover effects from market j to market i. Greenwood-Nimmo et al. (2015a) stress that, due to the order-invariance of GVDs, the variables in $\boldsymbol{y}_t$ can be re-ordered as

necessary to support any desired block structure.[4] Using this block structure, we may define the total within-market FEV contribution for market i as follows:

$$\mathcal{W}_{i\leftarrow i}^{(h)} = \frac{1}{m}\mathbf{e}_m'\mathbf{B}_{i\leftarrow i}^{(h)}\mathbf{e}_m \tag{10}$$

where $\mathbf{e}_m$ is a $m \times 1$ vector of ones. As such, $\mathcal{W}_{i\leftarrow i}^{(h)}$ measures the proportion of the h-step-ahead FEV of $\mathbf{y}_{it}$ explained by shocks to $\mathbf{y}_{it}$. $\mathcal{W}_{i\leftarrow i}^{(h)}$, can be decomposed into common-variable FEV contributions within market i, $\mathcal{O}_{i\leftarrow i}^{(h)}$ and cross-variable effects, $\mathcal{C}_{i\leftarrow i}^{(h)}$, as follows:

$$\mathcal{O}_{i\leftarrow i}^{(h)} = \frac{1}{m}\text{trace}\left(\mathbf{B}_{i\leftarrow i}^{(h)}\right) \text{ and } \mathcal{C}_{i\leftarrow i}^{(h)} = \mathcal{W}_{i\leftarrow i}^{(h)} - \mathcal{O}_{i\leftarrow i}^{(h)} \tag{11}$$

Note that $\mathcal{O}_{i\leftarrow i}^{(h)}$ measures the proportion of the h-step-ahead FEV of $\mathbf{y}_{it}$ which is not attributable to spillovers among the variables within market i nor to spillovers from other markets to market i. By contrast, $\mathcal{C}_{i\leftarrow i}^{(h)}$ records the total h-step-ahead spillover between the return, volatility and skewness within market i. Spillovers between markets i and j at horizon h are given by:

$$\mathcal{F}_{i\leftarrow j}^{(h)} = \frac{1}{m}\mathbf{e}_m'\mathbf{B}_{i\leftarrow j}^{(h)}\mathbf{e}_m \equiv \mathcal{T}_{i\leftarrow j}^{(h)} \text{ and } \mathcal{F}_{j\leftarrow i}^{(h)} = \frac{1}{m}\mathbf{e}_m'\mathbf{B}_{j\leftarrow i}^{(h)}\mathbf{e}_m \equiv \mathcal{T}_{j\leftarrow i}^{(h)} \tag{12}$$

and so we may define the $N \times N$ *market connectedness matrix* as:

$$\mathbb{M}^{(h)} = \begin{bmatrix} \mathcal{W}_{1\leftarrow 1}^{(h)} & \mathcal{F}_{1\leftarrow 2}^{(h)} & \dots & \mathcal{F}_{1\leftarrow N}^{(h)} \\ \mathcal{F}_{2\leftarrow 1}^{(h)} & \mathcal{W}_{2\leftarrow 2}^{(h)} & \dots & \mathcal{F}_{2\leftarrow N}^{(h)} \\ \vdots & \vdots & \ddots & \vdots \\ \mathcal{F}_{N\leftarrow 1}^{(h)} & \mathcal{F}_{N\leftarrow 2}^{(h)} & \dots & \mathcal{W}_{N\leftarrow N}^{(h)} \end{bmatrix} \tag{13}$$

It is now straightforward to construct aggregate spillover measures for market i as follows:

$$\mathcal{F}_{i\leftarrow \bullet}^{(h)} = \sum_{j=1,\neq i}^{N} \mathcal{F}_{i\leftarrow j}^{(h)} \text{ and } \mathcal{T}_{\bullet\leftarrow i}^{(h)} = \sum_{j=1,\neq i}^{N} \mathcal{T}_{j\leftarrow i}^{(h)} \tag{14}$$

[4] The block structure required to analyse connectedness among groups of common variables (i.e. returns for all markets, RNV innovations for all markets and RNS innovations for all markets) is outlined in **??**. In that specific case, one would reorder the variables in the VAR to obtain $\mathbf{y}_t = (\mathbf{r}_t, \mathbf{v}_t, \mathbf{s}_t)'$ where $\mathbf{r}_t = (r_{1t}, r_{2t}, \dots, r_{Nt})$, $\mathbf{v}_t = (v_{1t}, v_{2t}, \dots, v_{Nt})$ and $\mathbf{s}_t = (s_{1t}, s_{2t}, \dots, s_{Nt})$ and then aggregate into $g = 3$ groups of common variables each of which is composed of $m = N$ variables.

from which one can compute the net connectedness of market i, $\mathcal{N}_i^{(h)} = \mathcal{T}_{\bullet \leftarrow i}^{(h)} - \mathcal{F}_{i \leftarrow \bullet}^{(h)}$. The aggregate within-market effect and aggregate between-market spillover can be computed as:

$$\mathcal{H}^{(h)} = \frac{1}{N} \sum_{i=1}^{N} \mathcal{W}_{i \leftarrow i}^{(h)} \quad \text{and} \quad \mathcal{S}^{(h)} = \frac{1}{N} \sum_{i=1}^{N} \mathcal{F}_{i \leftarrow \bullet}^{(h)} = \frac{1}{N} \sum_{i=1}^{N} \mathcal{T}_{\bullet \leftarrow i}^{(h)}. \tag{15}$$

The generalisation of these results to measure the connectedness among the three variable groups in the model (returns for all markets, RNV innovations for all markets and RNS innovations for all markets) is straightforward and is discussed in **??**.

3. Dataset and Risk-Neutral Moments

Our model is estimated using daily returns and the innovations in RNV and RNS for the G10 currencies, with all quotes against the U.S. dollar.[5] We therefore work with the following nine currencies: the Australian dollar (AUD), the British pound (GBP), the Canadian dollar (CAD), the euro (EUR), the Japanese yen (JPY), the New Zealand dollar (NZD), the Norwegian krone (NOK), the Swedish krona (SEK) and the Swiss franc (CHF). Our sample spans the period since the introduction of the euro, from January 1999 to October 2014. We compute the daily return for the i-th currency as follows:

$$r_{it} = \ln(S_{it}) - \ln(S_{i,t-1}), \tag{16}$$

where S_{it} is the spot exchange rate in units of U.S. dollars per foreign currency unit and is sourced from WM/Reuters via Datastream. We compute the risk-neutral moments following the model-free framework developed by Breedon and Litzenberger (1978), Bakshi and Madan (2000), Carr and Madan (2001) and Bakshi et al. (2003), and applied to foreign exchange options by Jurek (2014). The computation requires appropriate forward exchange rate data, an annualised domestic interest rate and a set of at-the-money and out-of-the-money call and put options. We gather daily one month forward exchange rate data for each currency quoted against the U.S. dollar

[5] We also consider a model including innovations in risk-neutral kurtosis (RNK) but find this to yield little empirical benefit – see **??**. Full results are available on request. RNK is also found to be relatively unimportant in an empirical sense by Rafferty (2012). In general, to the extent that investors are concerned about mass in the tails of the expected distribution of future exchange rate changes, their preferences will tend to be strongly asymmetric and this will be captured by the RNS.

from WM/Reuters via Datastream. For the interest rate, we use daily data on U.S. eurocurrency interbank money market interest rates with a maturity of one month collected from the Financial Times and ICAP via Datastream. Finally, daily quotes for over-the-counter European FX options with a maturity of 1 month are provided by J.P. Morgan. The options data is quoted in the form of Garman and Kohlhagen (1983) implied volatilities for portfolios of out-of-the-money 25δ and 10δ options contracts as well as an at-the-money delta-neutral (0δ) straddle. From these, we extract the relevant strike prices and optionoptions pric prices using the Garman and Kohlhagen formulae. Using these, we then compute the model-free risk-neutral moments. A detailed discussion of the methods used in computing the risk-neutral moments is provided in **??**.

Following the approach adopted by Menkhoff et al. (2012) and Chang et al. (2013), we work with the innovations in RNV and RNS rather than their levels. The RNV and RNS innovations for the i-th market are extracted as the residuals from auxiliary first order autoregressions as follows:

$$v_{it} = \text{VOL}_{it}^{RN} - \widehat{\phi}_{iv}\text{VOL}_{i,t-1}^{RN} - \widehat{\mu}_{iv}, \tag{17}$$

$$s_{it} = \text{SKEW}_{it}^{RN} - \widehat{\phi}_{is}\text{SKEW}_{i,t-1}^{RN} - \widehat{\mu}_{is}, \tag{18}$$

where VOL_{it}^{RN} and SKEW_{it}^{RN} denote the option-implied risk-neutral volatility and skewness for currency i at time t, while Greek letters denote the estimated model parameters. The use of innovations allows us to account for the serial correlation in the risk-neutral moments without including a large number of lags in our VAR model. With fewer freely estimated parameters in the VAR model we can work with shorter rolling samples, allowing for richer patterns of time variation. In addition, working with innovations also has a theoretical advantage, as it allows us to focus on unexpected changes in RNV and RNS which reflect unexpected changes in the investment opportunity set facing investors.

Table 1 provides basic summary statistics for our dataset. All currencies in our sample except the GBP appreciated against the U.S. dollar during our sample, with the annualised rate of return over the full sample varying between -0.03% (GBP) and 2.4% (NZD). The standard deviation of the RNV innovations is largest for those currencies which are closely linked by carry trades, notably the JPY and AUD. Meanwhile, the GBP and the CAD are notable for the high degree of time variation in their RNS innovations. Time series plots of the data, provided in **??**, reveal

considerable commonality in the evolution of spot exchange rates for the European currencies reflecting their exposure to common influences. A marked spike in RNV is observed across all markets in September 2008 following the collapse of Lehman Brothers and a pronounced increase in the magnitude and volatility of RNS innovations is evident in many markets thereafter.

— Insert Table 1 about here —

4. Full-Sample Analysis

4.1. Connectedness among Variables over the Full Sample

To establish a point of reference, we first estimate a VAR(1) model over the full sample, where the VAR lag length is selected using the Schwarz criterion. In order to compute the connectedness matrix, one must choose an appropriate forecast horizon. However, as there is no simple method to select an optimal horizon, we experiment with $h \in \{5, 10, 15\}$, a range which encompasses the values used in the majority of the existing applications of the Diebold-Yilmaz framework to daily data. In practice, we find that the connectedness matrix is remarkably robust to the choice of forecast horizon. Indeed, the Frobenius norms for $\mathbb{C}^{(5)}$, $\mathbb{C}^{(10)}$ and $\mathbb{C}^{(15)}$ are 277.118, 277.117 and 277.117 respectively, indicating that the connectedness matrices are almost identical over the chosen range of forecast horizons. Closer inspection reveals that the degree of similarity is remarkable — if one compares $\mathbb{C}^{(5)}$ vs. $\mathbb{C}^{(10)}$ and $\mathbb{C}^{(10)}$ vs. $\mathbb{C}^{(15)}$ on an element-by-element basis, the largest absolute difference between a matching pair of elements is just 2.72×10^{-4}. We therefore adopt $h = 10$ throughout our full-sample analysis without loss of generality — we shall return to the issue of robustness in the context of rolling regression analysis in Section 5 below.

Table 2 presents the full-sample ten-days-ahead 27×27 variable connectedness matrix. Several features are noteworthy. Firstly, consider spillovers affecting returns. Own-variable effects exert a relatively weak influence on returns, typically accounting for 20–30% of the ten-days-ahead FEV. Over the full sample, we do not observe strong within-market spillovers from the RNV or RNS innovations of currency i to the return on currency i. The largest within-market spillovers onto returns are 10.9% and 5.9% in the case of RNV innovations for JPY and AUD respectively, with most being much smaller. The major force affecting the return FEV is spillovers between the

returns on different currencies, which account for more than 50% of the return FEV in most cases. Such strong cross-market spillovers are consistent with currency comovements driven by investors rebalancing positions in multiple currencies simultaneously in response to shocks, as documented by Elyasiani and Kocagil (2001), Cai et al. (2008) and Greenwood-Nimmo et al. (2015b).

— Insert Table 2 about here —

Spillovers among returns are particularly strong where currencies share an underlying linkage. This is particularly true for European currencies as well as the commodity currencies (AUD, NZD and CAD). Within these groups of currencies, many of the bilateral return spillovers are of the order of 10-15%. The own-variable effect for returns in conjunction with cross-market spillovers among returns collectively accounts for between 66% and 96% of return FEV. The JPY is a notable special case, displaying a considerably stronger own-variable effect than any other currency (52%) coupled with strong within-market spillovers from RNV and RNS innovations. Meanwhile, cross-market return spillovers from other currencies account for a mere 14% of the JPY return FEV. The relative disconnect of JPY returns from the returns of other currencies provides support for the notion that the JPY is a safe haven currency (Ranaldo and Söderlind, 2010).

Similar features characterise RNV innovations. Own-variable effects account for between 17% (EUR) and 27% (JPY) of the ten-days-ahead FEV, with an average value of 20%. As with returns, we observe relatively mild within-market spillovers onto RNV innovations juxtaposed with very strong spillovers between RNV innovations across currencies, ranging from 59% (JPY) to 77% (EUR). In total, the own-variable effect for RNV innovations and cross-market spillovers among RNV innovations account for between 83% and 94% of the ten-days-ahead FEV. This suggests that uncertainty spreads rapidly and forcefully among FX markets in line with the distinguished literature on volatility transmission (e.g. Engle et al., 1990; Fleming et al., 1998) and points to the role of a global FX volatility factor in driving the RNV innovations of individual currencies (Menkhoff et al., 2012). As with return spillovers, strong volatility spillovers are evident between currencies that share an underlying linkage. The safe haven status of the JPY is again apparent, with the JPY being less susceptible to cross-market RNV spillovers than other currencies.

RNS innovations experience considerably stronger own-variable effects than either returns or

RNV innovations and, by construction, commensurately weaker spillovers from the system. There is marked heterogeneity across markets, with the own-variable effects for RNS innovations varying in the range 64% (NZD) to 91% (CAD) and taking an average value of 76%. Currencies' upside and downside crash risks are more strongly influenced by currency-specific idiosyncratic shocks than is the case for either returns or RNV innovations. This is in line with the limited literature on skewness spillovers in equity markets, which emphasises the role of local factors (Hashmi and Tay, 2007, 2012). Nevertheless, more closely related currency pairs exhibit stronger skewness spillovers — for example the NOK/SEK and AUD/NZD pairs — which suggests that exposure to common shocks may induce a degree of common crash risk.

4.2. Full-Sample Market and Moment Connectedness Matrices

Over the full-sample, it is possible to meaningfully interpret the 729 elements of the 27x27 variable connectedness matrix shown in Table 2. However, this rapidly becomes burdensome when working with subsamples and wholly infeasible in the context of rolling regression analysis. As noted above, block aggregations of the connectedness matrix may be used to focus the analysis as desired. We briefly consider two cases here, both of which will be used extensively in the rolling-sample analysis below. Table 3 presents the 9×9 market connectedness matrix, which is given by Equation (13). Adopting the nomenclature proposed by Engle et al. (1990), the within-market effects recorded on the prime-diagonal of this matrix can be thought of as heatwave effects while the cross-market spillovers are akin to meteor showers. Presenting the market connectedness matrix in this way highlights the key interactions among markets noted above. In the majority of markets, the heatwave effect accounts for less than 50% of the FEV and spillovers from other markets typically exert a dominant influence. Currencies which share an underlying linkage experience stronger bilateral spillovers and the safe haven status of the JPY is easily seen.

— Insert Table 3 about here —

Similarly, Table 4 reports the 3×3 moment connectedness matrix which measures the full-sample connectedness among returns, RNV and RNS innovations aggregated over all 9 markets. This representation of the connectedness matrix focuses attention on the observation that spillovers

among variables of the same type (e.g. spillovers among returns or spillovers among RNV innovations) are by the far the dominant force in the system over the full sample, accounting for more than 80% of FEV in each case. Nonetheless, spillovers between returns, RNV innovations and RNS innovations are non-negligible, implying that there exists a bidirectional relationship where returns adjust in response to the option-implied moments and vice-versa.

— Insert Table 4 about here —

5. Rolling-Sample Analysis

With the full-sample benchmark in place, we now consider time-varying connectedness by means of rolling regression analysis. Given that there is as yet no robust consensus in the literature regarding the appropriate choice of window length, we start by considering candidate values in the set $w \in \{200, 250, 300\}$ trading days. Furthermore, we consider candidate forecast horizons in the set $h \in \{5, 10, 15\}$ trading days to verify that the robustness of our full-sample results to the choice of forecast horizon also carries over to rolling-sample analysis. Lastly, for completeness, we also investigate the effect of using orthogonalised forecast error variance decompositions (OVDs) under 1,000 random variable orderings as opposed to GVDs (see Diebold and Yilmaz, 2014, for a similar exercise).[6]

— Insert Figure 1 about here —

Examining Figure 1 reveals that neither the choice of forecast horizon nor of window length exerts a significant influence over our results. The time series behaviour of the aggregate spillover index, based on Equation (8), is remarkably similar in all cases. Furthermore, the spillover indices based on OVDs and GVDs track one-another closely, with the correlation between the spillover indices based on GVDs and the mean of the spillover indices based on OVDs being no lower than 0.95 in any case. The main difference between the GVD and OVD results is a slight level shift. Diebold and Yilmaz (2014, p. 130) observe the same effect and note that the aggregate spillover

[6]Full-sample connectedness matrices corresponding to Tables 2–4 computed using OVDs are not reported here in order to conserve space but they are available on request.

activity computed using OVDs acts as a lower bound on that derived from GVDs. The GVD results may be considered more accurate because, unlike OVDs, GVDs accommodate the full correlation structure of the reduced form VAR disturbances.

5.1. Aggregate Spillover Activity over Time

In light of Figure 1, the remainder of our analysis focuses on the GVD case with $w = 250$ and $h = 10$ trading days, which corresponds to the central panel of the figure. Figure 2 shows the aggregate spillover index in this case, enlarged and annotated with the timing of several major events. Spillovers begin to rise in late 2000 following the collapse of the dotcom bubble and the ensuing U.S. recession. They continue to rise during the Federal Reserve's monetary accommodation from 2001–4. Spillover activity then gradually recedes with the normalisation of U.S. interest rates until the onset of the subprime mortgage crisis in 2007, with a particularly rapid intensification of spillover activity following the collapse of Lehman Brothers in September 2008. Spillovers remain at a high level during the GFC and for several years thereafter during the sovereign debt crisis before receding in late 2012 with the gradual abatement of the sovereign debt crisis.

— Insert Figure 2 about here —

5.2. Connectedness among Markets over Time

Figure 3 summarises the time-varying connectedness among markets. The figure is composed of nine panels, one for each market. The panel for the ith market is divided into an upper plot showing the within-market heatwave effect, $\mathcal{W}_{i\leftarrow i}^{(10)}$ and a lower plot showing the outward and inward spillovers for market i, $\mathcal{T}_{\bullet\leftarrow i}^{(10)}$ and $\mathcal{F}_{i\leftarrow\bullet}^{(10)}$, respectively. Recall that $\mathcal{T}_{\bullet\leftarrow i}^{(10)}$ may exceed 100% by virtue of its construction following Equation (14).

— Insert Figure 3 about here —

The figure is laid out such that currencies which display similar behaviour appear in the same row. Consider the top row, which contains the AUD, NZD and CAD, each of which is a commodity currency. In each case, the within-market effect is very high at the start of the sample, accounting for approximately 70% of market FEV, which indicates strong idiosyncratic variation and relatively

weak integration with the other markets in the system. However, this changes markedly over the sample period and within-market effects drop to around 30% during the GFC. Between-market spillover activity — both inward and outward — increases markedly at this time, reflecting much greater integration of the commodity currencies with the system as a whole. This is an intuitive finding as commodity currencies are known to be sensitive to global economic performance.

The European currencies (EUR, NOK, SEK) appear on the middle row. Along with the CHF, these display common behaviour, with generally low within-market (idiosyncratic) effects throughout the sample matched by strong between-market spillovers. The positive net spillovers arising from the EUR and the CHF over much of the sample suggest that these are the leading European markets, as one may expect. Finally, the GBP and JPY display a degree of common behaviour. Both maintain somewhat higher within-market spillovers over the sample than the majority of the other currencies and neither exhibits strong inward or outward between-market spillovers, which suggests that both markets may provide a safe haven for FX investors.

5.3. Connectedness among Moments over Time

Figure 4 reports a simple decomposition of the moment connectedness matrix over rolling samples. The figure contains nine panels, each of which contains two plots. The upper plot shows the connectedness among moments within the same market and the lower plot shows the connectedness among moments between markets.[7] Focus initially on the upper row of the figure, which reports the evolution of the spillovers affecting returns over our sample period. As with the full-sample results documented above, the own-variable within-market effect in returns — i.e. the average of the diagonal elements within the upper left block of (B.1) — is relatively weak, always remaining below 40% and declining substantially during the GFC. Spillovers among returns between markets are much stronger in general, peaking at 68% in 2005 before dipping during the GFC. Meanwhile, spillovers to returns from RNV and RNS innovations increase substantially during the GFC and the European sovereign debt crisis, reaching a high of nearly 50% combined

[7] The aggregation routine used in the computation of Figure 4 is recorded in **??**. Note that the figure is laid out such that it maps on to the block structure of Equation (B.1). The within-market effects plotted in the figure are computed as the average of the diagonal elements of the relevant block in Equation (B.1) while the between-market effects are computed as the sum of the off-diagonal elements in the relevant block divided by the number of currency markets.

in October 2008, shortly after the collapse of Lehman Brothers. This indicates a marked increase in investors' sensitivity to risk during the crises. Furthermore, given that the large majority of spillovers to returns from RNV and RNS innovations occurs between markets, one may infer that investors were particularly concerned with systematic risk (aggregate FX uncertainty and crash risk in particular).

— Insert Figure 4 about here —

The second row of Figure 4 focuses on spillovers affecting RNV innovations. As with returns, the own-variable within-market effect in RNV innovations is relatively weak and has gradually fallen across our sample. By contrast, between-market spillovers among RNV innovations have gradually intensified from roughly 50% at the start of our sample to more than 65% towards the end of the sample, indicating that systematic volatility linkages dominate the effect of idiosyncratic volatility. Cross-market spillovers from returns to RNV innovations strengthen considerably in the aftermath of the GFC and during the European sovereign debt crisis. This indicates that investors' forward-looking perceptions of exchange rate volatility are increasingly conditioned on realised exchange rate movements.

The last row of Figure 4 reveals that the own-variable within-market effect in RNS innovations is much stronger than is the case with either returns or RNV innovations. Furthermore, it displays marked time variation, reflecting the importance of currency-specific influences on RNS innovations. Interestingly, the own-variable effect for RNS innovations falls dramatically during the GFC and European debt crisis, more than halving from 50% to less than 25%. This is mirrored by an increase in between-market spillovers among RNS innovations. The intensification of skewness spillovers across markets during turbulent times suggests that coordinated crash risk is more prevalent during times of financial stress, as the likelihood of carry trade positions having to be unwound due to liquidity constraints increases (e.g. Brunnermeier et al., 2009; Rafferty, 2012). Finally, we also observe a large increase in spillovers from returns to RNS innovations during the GFC and the European sovereign debt crisis, which indicates that investors' forward-looking perceptions of crash risk are heavily conditioned on realised exchange rate movements, as one may expect.

6. Relationship to Macroeconomic and Financial Conditions

Careful consideration of our rolling-sample results suggests two interesting phenomena which may be discerned most easily in relation to the aggregate spillover index in Figure 2. First, it appears that FX spillovers evolve countercyclically. Second, FX spillovers seem to intensify in times of financial stress, suggesting a greater role of currency-specific idiosyncratic factors in tranquil times and of common systematic factors in times of stress. Both effects are demonstrated in Figure 5, which plots the rolling spillover index shown in Figure 2 alongside the 250-day rolling average of the Federal funds rate, the TED spread and the VIX, respectively. The use of rolling averages provides a measure of the low frequency movements of each series which lends itself to a medium- or long-term interpretation.

— Insert Figure 5 about here —

The federal funds rate is a gauge of the cyclical position of the U.S. economy. The figure shows a remarkably strong negative relationship between FX spillovers and the federal funds rate. The correlation is -0.54 over the full sample and -0.71 in the period up to December 2008 when active interest rate policy was curtailed by the zero lower bound (ZLB). This striking correlation is suggestive of a possible U.S. dollar factor driving exchange rate dynamics and linkages in the foreign exchange markets (Lustig et al., 2011). The central panel of Figure 5 shows the relationship between FX spillovers and the TED spread. While not as strong as the relationship with the federal funds rate, there is a positive correlation over the full sample of 0.11. Furthermore, the positive relationship strengthens during and after the GFC, with a correlation of 0.42 since September 2008. This indicates that FX spillovers tend to intensify during periods of illiquidity. The bottom panel of Figure 5 reveals that FX spillovers are positively correlated with the VIX. The correlation over the full sample is 0.33 and this positive correlation strengthens to 0.75 since September 2008. This indicates that FX spillovers tend to intensify during periods of financial stress.

To complement the preceding low frequency analysis, we test whether large changes in the value of the spillover index occur in conjunction with large changes to the federal funds rate, the TED spread or the VIX. To this end, we construct the following binary indicators to identify periods in

which the spillover index reaches a new 250-day high or low, respectively:

$$\overline{S_t} = \mathbb{1}\Big\{S_t^{(h)} - \max\left(S_{t-1}^{(h)}, \ldots, S_{t-250}^{(h)}\right) > 0\Big\} \quad \& \quad \underline{S_t} = \mathbb{1}\Big\{S_t^{(h)} - \min\left(S_{t-1}^{(h)}, \ldots, S_{t-250}^{(h)}\right) < 0\Big\}$$

where $\mathbb{1}\{\cdot\}$ is a Heaviside step function which takes the value one if the condition in braces is satisfied and zero otherwise. We apply the same procedure to define 250-day high and low indicator variables for the federal funds rate ($\overline{F_t}$ and $\underline{F_t}$), the TED spread ($\overline{T_t}$ and $\underline{T_t}$) and the VIX ($\overline{V_t}$ and $\underline{V_t}$). We then use these indicators to compute an array of pseudo-hit-rates. For example, the pseudo-hit-rate capturing occasions on which the spillover index records a new 250-day high *and* the federal funds rate records a new 250-day low within ±5 days is given by:

$$\mathbb{H}\left(\overline{S_t}, \underline{F_t}\right) = \left(\frac{\sum_{t=w+1}^{T} \mathbb{1}\left\{\left(\overline{S_t} \times \sum_{i=-5}^{5} \underline{F_{t+i}}\right) \neq 0\right\}}{\sum_{t=w+1}^{T} \overline{S_t}}\right) \times 100\% \tag{19}$$

In light of Figure 5, given that we expect that changes in the spillover index are negatively correlated with the federal funds rate and positively correlated with the TED spread and the VIX, we compute the following pseudo-hit-rates: $\mathbb{H}\left(\overline{S_t}, \underline{F_t}\right)$, $\mathbb{H}\left(\underline{S_t}, \overline{F_t}\right)$, $\mathbb{H}\left(\overline{S_t}, \overline{T_t}\right)$, $\mathbb{H}\left(\underline{S_t}, \underline{T_t}\right)$, $\mathbb{H}\left(\overline{S_t}, \overline{V_t}\right)$ and $\mathbb{H}\left(\underline{S_t}, \underline{V_t}\right)$. The results are reported in Table 5, while Figure 6 records the timing of the respective hits.

— Insert Table 5 and Figure 6 about here —

The hit-rate with respect to the federal funds rate is relatively high over the full sample despite the ZLB constraint which has seen relative constancy of the funds rates since December 2008. When considered only over the pre-ZLB period, the hit rate is quite remarkable, with 62% of spillover highs occurring within ±5 days of a funds rate low and 35% of spillover lows within ±5 days of a funds rate high. These results indicate that FX market participants respond rapidly to signals arising from U.S. monetary policy, particularly where the signal is of a deterioration in U.S. macroeconomic and financial conditions.

Hit-rates with respect to the TED spread and the VIX are relatively low over the full sample but are much higher in the period of financial turbulence since the collapse of Lehman Brothers. This is particularly true of the VIX, where almost half of all spillover highs occur within ±5 days of a corresponding VIX high and a third of spillover lows correspond to a VIX low. Furthermore,

Figure 6 suggests that hits with respect to the TED spread occur only during periods where the spillover index is either rising or falling particularly dramatically, suggesting that such large swings in spillover activity may be driven by liquidity effects. The overall implication is that FX market participants respond more rapidly to bad news than to good news, as one may expect in light of the literature documenting asymmetric responses to positive and adverse shocks in a variety of contexts including the well-known equity leverage effect.

7. Conclusion

We study the interaction between FX returns and the innovations in the option-implied RNV and RNS for the G10 currencies. Our use of risk-neutral moments accords with recent developments in the literature, which stress their benefits over realised risk measures in terms of their forward-looking nature and their model-free computation (Bakshi and Madan, 2000; Carr and Madan, 2001; Bakshi et al., 2003). Our analysis is based on the connectedness methodology recently advanced by Diebold and Yilmaz (2009, 2014).

Several interesting results emerge from our analysis. Firstly, over the full sample period, we observe strong spillovers among returns, with particularly notable bilateral spillovers among currencies which share an underlying linkage, such as those which are exposed to common shocks. Similarly, spillovers among RNV innovations across currencies account for as much as 75% of the ten-days-ahead FEV of RNV innovations, indicating that systematic volatility plays a dominant role while idiosyncratic volatility is much less important on average. However, over the full sample, the opposite is true of RNS innovations, where idiosyncratic factors play an important role in driving measures indicating the risk of large jumps and crashes in exchange rates.

Rolling-sample analysis reveals significant time variation in both the pattern and intensity of spillovers. A general tendency towards increased spillovers among markets during the GFC and the sovereign debt crisis is apparent, with the JPY and GBP remaining somewhat insulated from the other markets and, therefore, providing a safe haven for FX investors. Importantly, this increase in interdependence arises among returns as well as innovations in RNV and RNS, which implies a degree of common behaviour of realised returns and also of forward-looking measures of risk. Importantly, we find that spillovers of RNS innovations between markets intensify particularly

markedly at this time, highlighting the key role of crash risk — and of coordinated crash risk in particular — during the crises. Finally, we demonstrate that spillover activity among FX markets evolves countercyclically, rising during periods of financial stress and also rising when domestic conditions in the U.S. deteriorate. The development of models to explore the causes and consequences of these changing patterns of spillover behaviour represents a fruitful avenue for continuing research.

Acknowledgements

We are indebted to J.P. Morgan and to Raphael Brun-Aguerre in particular for providing the FX options data used to compute the risk-neutral moments. We are grateful for the helpful discussion of Heather Anderson, Efrem Castelnuovo, Yu-chin Chen, Chris Neely, Kalvinder Shields, Yongcheol Shin, Chris Skeels and Vance Martin and for the comments of participants at the First Conference on Recent Developments in Financial Econometrics and Applications (Deakin University, December 2014) and of seminar participants at the University of Auckland. Financial support from the Faculty of Business and Economics at the University of Melbourne is gratefully acknowledged. The usual disclaimer applies.

References

Ang, A., Hodrick, R. J., Xing, Y., Zhang, X., 2006. The Cross-Section of Volatility and Expected Returns. Journal of Finance 61, 259–299.

Ang, A., Hodrick, R. J., Xing, Y., Zhang, X., 2009. High Idiosyncratic Volatility and Low Returns: International and Further US Evidence. Journal of Financial Economics 91, 1–23.

Bakshi, G., Kapadia, N., Madan, D., 2003. Stock Return Characteristics, Skew Laws and the Differential Pricing of Individual Equity Options. Review of Financial Studies 16, 101–143.

Bakshi, G., Madan, D., 2000. Spanning and Derivative-Security Valuation. Journal of Financial Economics 55, 205–238.

Bakshi, G., Panayotov, G., 2013. Predictability of Currency Carry Trades and Asset Pricing Implications. Journal of Financial Economics 110 (1), 139–163.

Billio, M., Getmansky, M., Lo, A., Pelizzon, L., 2012. Econometric Measures of Connectedness and Systemic Risk in the Finance and Insurance Sectors. Journal of Financial Economics 104, 535–559.

Breedon, D., Litzenberger, R., 1978. Prices of State-Contingent Claims Implicit in Option Prices. Journal of Business, 617–651.

Brunnermeier, M. K., Nagel, S., Pedersen, L. H., 2009. Carry Trades and Currency Crashes. NBER Macroeconomics Annual 2008 23, 313–347.

Bubák, V., Kočenda, E., Žikeš, F., 2011. Volatility Transmission in Emerging European Foreign Exchange Markets. Journal of Banking and Finance 35, 2829–2841.

Burnside, C., Eichenbaum, M., Kleshchelski, I., Rebelo, S., 2011. Do Peso Problems Explain the Returns to the Carry Trade? Review of Financial Studies 24, 853–891.

Cai, F., Howorka, E., Wongswan, J., 2008. Informational Linkage Across Trading Regions: Evidence from Foreign Exchange Markets. Journal of International Money and Finance 27, 1212–1243.

Carr, P., Madan, D., 2001. Optimal Positioning in Derivative Securities. Quantitative Finance 1, 19–37.

Castagna, A., Mercurio, F., 2007. The Vanna-Volga Method for Implied Volatilities. Risk 20, 106–111.

Chang, B. Y., Christoffersen, P., Jacobs, K., 2013. Market Skewness Risk and the Cross-Section of Stock Returns. Journal of Financial Economics 107, 46–68.

Chen, Y.-C., Gwati, R., 2014. Understanding Exchange Rate Dynamics: What does the Term Structure of FX Options Tell Us? Mimeo, Washington University.

Christoffersen, P., Jacobs, K., Chang, B. Y., 2013. Forecasting with Option-Implied Information. In: Elliott, G., Timmermann, A. (Eds.), Handbook of Economic Forecasting. Vol. 2A. North-Holland, Amsterdam, pp. 581–656.

Conrad, J., Dittmar, R. F., Ghysels, E., 2013. Ex Ante Skewness and Expected Stock Returns. The Journal of Finance 68, 85–124.

Diebold, F., Yilmaz, K., 2009. Measuring Financial Asset Return and Volatility Spillovers, with Application to Global Equity Markets. Economic Journal 119, 158–171.

Diebold, F., Yilmaz, K., 2014. On the Network Topology of Variance Decompositions: Measuring the Connectedness of Financial Firms. Journal of Econometrics 182, 119–134.

Elyasiani, E., Kocagil, A., 2001. Interdependence and Dynamics in Currency Futures: A Multivariate Cointegration Analysis of Intra-day Data. Journal of Banking and Finance 25, 1161–1186.

Engle, R. F., Ito, T., Lin, W.-L., 1990. Meteor Showers or Heat Waves? Heteroskedastic Intra-daily Volatility in the Foreign Exchange Market. Econometrica 58, 525–524.

Farhi, E., Fraiberger, S. P., Gabaix, X., Rancier, R., Verdelhan, A., 2014. Crash Risk in Currency Markets. Mimeo, Massachusetts Institute of Technology.

Fleming, J., Kirby, C., Ostdiek, B., 1998. Information and Volatility Linkages in the Stock, Bond, and Money Markets. Journal of Financial Economics 49, 111–137.

Garman, M. B., Kohlhagen, S. W., 1983. Foreign Currency Option Values. Journal of International Money and Finance 2, 231–237.

Greenwood-Nimmo, M. J., Nguyen, V. H., Shin, Y., 2015a. Measuring the Connectedness of the Global Economy. Mimeo, University of Melbourne.

Greenwood-Nimmo, M. J., Nguyen, V. H., Shin, Y., 2015b. Quantifying Informational Linkages in a Global Model of Currency Spot Markets. Mimeo, University of Melbourne.

Hashmi, A. R., Tay, A. S., 2007. Global Regional Sources of Risk in Equity Markets: Evidence from Factor Models with Time-Varying Conditional Skewness. Journal of International Money and Finance 26, 430–453.

Hashmi, A. R., Tay, A. S., 2012. Mean, Volatility and Skewness Spillovers in Equity Markets. In: Bauwens, L., Hafner, C., Laurent, S. (Eds.), Handbook of Volatility Models and Their Applications, 1st Edition. John Wiley and Sons, Ch. 5, pp. 127–145.

Hong, Y., 2001. A Test for Volatility Spillover with Application to Exchange Rates. Journal of Econometrics 103 (1), 183–224.

Jiang, G. J., Tian, Y. S., 2005. The Model-Free Implied Volatility and its Information Content. Review of Financial Studies 18, 1305–1342.

Jurek, J. W., 2014. Crash-Neutral Currency Carry Trades. Journal of Financial Economics 113, 325–347.

Kearney, C., Patton, A. J., 2000. Multivariate GARCH Modeling of Exchange Rate Volatility Transmission in the European Monetary System. Financial Review 35 (1), 29–48.

Lustig, H., Roussanov, N., Verdelhan, A., 2011. Common Risk Factors in Currency Markets. Review of Financial Studies 24, 3731–3777.

Melvin, M., Melvin, B. P., 2003. The Global Transmission of Volatility in the Foreign Exchange Market. Review of Economics and Statistics 85 (3), 670–679.

Menkhoff, L., Sarno, L., Schmeling, M., Schrimpf, A., 2012. Carry Trades and Global Foreign Exchange Volatility. The Journal of Finance 67, 681–718.

Nikkinen, J., Sahlström, P., Vähämaa, S., 2006. Implied Volatility Linkages among Major European Currencies. Journal of International Financial Markets, Institutions and Money 16 (2), 87–103.

Pesaran, M., Shin, Y., 1998. Generalized Impulse Response Analysis in Linear Multivariate Models. Economics Letters 58, 17–29.

Rafferty, B., 2012. Currency Returns, Skewness and Crash Risk. Mimeo, University of Melbourne.

Ranaldo, A., Söderlind, P., 2010. Safe Haven Currencies. Review of Finance 14, 385–407.

		AUD	CAD	EUR	JPY	NZD	NOK	SEK	CHF	GBP
Spot Rate	Mean	0.783	0.840	1.225	0.010	0.657	0.152	0.133	0.852	1.662
	Std Dev	0.168	0.136	0.183	0.001	0.136	0.023	0.019	0.178	0.169
Annualised	Mean	0.022	0.019	0.005	0.003	0.024	0.009	0.007	0.022	-0.003
Return	Std Dev	0.131	0.091	0.099	0.103	0.135	0.119	0.120	0.107	0.091
Volatility	Mean	0.122	0.090	0.106	0.111	0.133	0.121	0.123	0.109	0.093
	Std Dev	0.048	0.035	0.033	0.034	0.042	0.037	0.038	0.028	0.033
Volatility	Mean	0.000	0.000	0.000	0.000	0.000	0.000	0.000	0.000	0.000
Innovations	Std Dev	0.006	0.004	0.004	0.006	0.006	0.004	0.004	0.005	0.004
Skewness	Mean	-0.193	-0.478	-0.232	0.050	-0.122	-0.078	-0.169	-0.260	-0.303
	Std Dev	0.334	0.477	0.428	0.445	0.292	0.277	0.240	0.359	0.448
Skewness	Mean	0.000	0.000	0.000	0.000	0.000	0.000	0.000	0.000	0.000
Innovations	Std Dev	0.087	0.118	0.092	0.118	0.061	0.076	0.081	0.113	0.149

NOTES: Although daily returns are used in estimation, statistics for the annualised returns are reported for ease of interpretation. Following Menkhoff et al. (2012) and Chang et al. (2013), the innovations in risk-neutral volatility and skewness are recovered as the residuals from auxiliary AR(1) models as documented in equations (17) and (18).

Table 1: Full Sample Descriptive Statistics

		AUD			CAD			EUR			JPY			NZD			NOK			SEK			CHF			GBP		
		r	v	s	r	v	s	r	v	s	r	v	s	r	v	s	r	v	s	r	v	s	r	v	s	r	v	s
AUD	r	20.4	5.9	1.2	7.8	2.8	0.2	6.2	1.7	0.2	0.0	2.0	0.0	14.1	5.0	1.5	7.2	1.6	0.2	7.4	1.6	0.1	3.3	1.3	0.0	5.9	2.3	0.1
	v	5.4	18.7	0.1	2.0	7.5	0.0	0.8	7.3	0.0	0.8	6.2	0.1	3.5	15.5	0.3	1.5	7.0	0.0	1.2	6.7	0.0	0.1	6.4	0.0	1.3	7.3	0.1
	s	4.6	0.6	69.9	1.9	0.5	0.4	1.8	0.1	0.4	0.0	0.2	0.0	3.5	0.6	5.5	2.1	0.1	1.5	2.0	0.1	1.0	0.9	0.1	0.5	1.3	0.2	0.2
CAD	r	11.3	3.1	0.8	29.8	3.6	0.6	6.0	1.1	0.2	0.0	1.0	0.0	9.0	2.7	0.9	7.8	1.2	0.1	7.9	1.1	0.1	3.2	0.8	0.0	5.8	1.7	0.0
	v	3.2	9.5	0.1	2.9	23.9	0.1	0.4	8.4	0.0	0.8	5.0	0.1	2.2	8.2	0.3	1.4	8.0	0.0	1.1	7.9	0.0	0.0	7.7	0.0	1.0	7.5	0.1
	s	0.7	0.0	0.6	1.6	0.4	91.3	0.7	0.1	0.3	0.2	0.1	0.1	0.6	0.0	0.1	0.5	0.1	0.1	0.5	0.1	0.1	0.6	0.1	0.1	0.5	0.1	0.3
EUR	r	6.5	0.9	0.4	4.3	0.4	0.2	21.2	0.4	1.2	1.3	0.0	0.1	6.2	0.8	0.6	14.0	0.4	0.4	14.7	0.3	0.3	15.1	0.2	0.2	9.4	0.5	0.1
	v	1.4	6.4	0.0	0.6	5.7	0.0	0.3	16.5	0.1	0.8	4.6	0.1	1.0	5.6	0.0	0.6	15.7	0.0	0.5	15.5	0.0	0.0	14.4	0.0	0.4	9.3	0.2
	s	0.8	0.1	0.2	0.5	0.2	0.2	4.4	0.3	72.6	0.5	0.5	0.1	0.8	0.0	0.4	2.7	0.3	1.1	2.7	0.3	1.3	3.5	0.5	1.8	1.8	0.1	2.0
JPY	r	0.0	2.2	0.0	0.0	1.8	0.1	3.1	2.4	0.3	52.4	10.9	4.4	0.1	2.0	0.0	1.4	2.4	0.0	1.2	2.4	0.0	7.1	2.4	0.1	1.0	2.1	0.3
	v	2.6	8.9	0.1	1.0	5.6	0.0	0.0	7.6	0.2	5.6	27.1	0.6	1.8	7.7	0.1	0.2	7.5	0.0	0.2	7.2	0.0	0.4	7.0	0.1	0.4	7.7	0.2
	s	0.0	0.3	0.0	0.0	0.4	0.1	0.4	0.6	0.1	7.5	1.8	82.1	0.0	0.4	0.3	0.1	0.6	0.0	0.1	0.6	1.2	0.9	0.7	0.9	0.1	0.4	0.1
NZD	r	15.8	4.3	0.9	6.9	2.2	0.1	6.7	1.4	0.3	0.0	1.5	0.0	22.9	4.3	1.7	7.4	1.4	0.2	7.4	1.3	0.1	3.7	1.1	0.0	6.5	1.9	0.1
	v	4.9	16.7	0.1	2.0	6.9	0.0	0.8	6.8	0.0	0.8	5.8	0.1	3.9	20.1	0.4	1.6	6.7	0.0	1.2	6.3	0.0	0.1	6.0	0.0	1.4	7.5	0.1
	s	5.2	1.2	5.3	2.3	0.8	0.1	2.3	0.2	0.1	0.0	0.3	0.2	5.3	1.5	63.9	2.7	0.2	0.6	2.9	0.2	1.4	1.1	0.2	0.0	1.5	0.2	0.2
NOK	r	7.6	1.7	0.6	5.6	1.2	0.1	14.1	0.7	0.7	0.6	0.2	0.0	6.9	1.7	0.8	21.4	0.7	0.3	14.8	0.7	0.3	9.5	0.6	0.1	8.1	1.0	0.1
	v	1.4	6.3	0.0	0.7	5.6	0.0	0.3	16.0	0.1	0.8	4.6	0.1	1.0	5.5	0.0	0.6	16.8	0.0	0.5	15.9	0.0	0.0	13.9	0.0	0.5	9.2	0.2
	s	0.5	0.1	1.4	0.3	0.1	0.1	1.6	0.1	1.1	0.0	0.0	0.0	0.5	0.1	0.6	1.1	0.1	68.0	1.2	0.1	17.5	0.9	0.0	3.8	0.7	0.0	0.1
SEK	r	7.8	1.4	0.5	5.7	1.0	0.1	15.0	0.6	0.8	0.5	0.2	0.0	6.9	1.2	0.8	14.9	0.6	0.4	21.6	0.6	0.3	9.6	0.4	0.1	8.1	0.8	0.1
	v	1.3	6.1	0.0	0.6	5.6	0.0	0.3	16.1	0.1	0.8	4.6	0.1	0.9	5.3	0.0	0.5	16.2	0.0	0.5	17.2	0.0	0.0	14.0	0.0	0.4	9.1	0.2
	s	0.4	0.1	1.0	0.2	0.0	0.1	1.4	0.0	1.3	0.0	0.1	0.8	0.5	0.0	1.2	0.9	0.0	16.9	1.1	0.0	68.4	0.9	0.1	3.8	0.7	0.0	0.1
CHF	r	4.4	0.1	0.3	2.9	0.0	0.2	19.6	0.0	1.2	3.8	0.4	0.3	4.5	0.1	0.4	12.2	0.0	0.3	12.4	0.0	0.3	27.6	0.2	0.2	8.4	0.0	0.2
	v	1.2	6.2	0.0	0.5	5.7	0.0	0.2	15.7	0.1	0.9	4.7	0.2	0.9	5.4	0.0	0.5	15.0	0.0	0.3	14.8	0.0	0.2	18.1	0.1	0.3	8.7	0.3
	s	0.2	0.0	0.7	0.1	0.0	0.1	0.8	0.2	2.0	0.1	0.2	0.5	0.2	0.0	0.0	0.5	0.1	4.4	0.5	0.1	4.5	1.0	0.4	82.8	0.3	0.1	0.2
GBP	r	7.7	1.8	0.5	5.2	1.1	0.2	11.8	0.7	0.6	0.5	0.4	0.0	7.5	1.8	0.6	10.1	0.7	0.2	10.0	0.7	0.2	8.1	0.5	0.1	26.5	2.4	0.2
	v	2.3	7.8	0.0	1.2	6.3	0.0	0.5	11.3	0.0	0.8	5.6	0.1	1.6	7.4	0.0	0.9	11.0	0.0	0.8	10.6	0.0	0.0	9.6	0.0	1.9	19.9	0.3
	s	0.2	0.3	0.3	0.1	0.3	0.4	0.7	1.1	2.1	0.4	0.7	0.1	0.3	0.3	0.2	0.6	1.0	0.1	0.5	1.0	0.1	0.8	1.2	0.2	0.8	1.3	84.7

NOTES: The connectedness matrix is computed using normalised generalised forecast error variance decompositions following Diebold and Yilmaz (2014). All values are measured in percentage points such that each row sums to 100% by construction. The depth of shading reflects the strength of the associated heatwave/spillover effect, with darker shading indicating a stronger effect.

Table 2: Full-Sample Connectedness among Variables, Ten-Days Ahead

	AUD	CAD	EUR	JPY	NZD	NOK	SEK	CHF	GBP
AUD	42.27	7.68	6.18	3.12	16.52	7.11	6.69	4.22	6.22
CAD	9.79	51.42	5.73	2.47	8.03	6.40	6.27	4.18	5.70
EUR	5.59	4.04	39.02	2.68	5.16	11.73	11.92	11.90	7.97
JPY	4.73	3.05	4.92	64.12	4.15	4.08	4.30	6.54	4.10
NZD	18.17	7.13	6.21	2.94	41.30	6.91	6.91	4.05	6.39
NOK	6.51	4.55	11.55	2.13	5.70	36.33	16.98	9.62	6.64
SEK	6.20	4.46	11.83	2.35	5.65	16.84	36.51	9.65	6.51
CHF	4.37	3.19	13.30	3.64	3.83	11.00	11.00	43.51	6.16
GBP	6.98	4.93	9.63	2.91	6.53	8.19	7.96	6.84	46.01

NOTE: The connectedness matrix is computed using normalised generalised forecast error variance decompositions following Diebold and Yilmaz (2014) under the block aggregation routine devised by Greenwood-Nimmo et al. (2015a). All values are measured in percentage points such that each row sums to 100% by construction. The depth of shading reflects the strength of the associated heatwave/spillover effect, with darker shading indicating a stronger effect.

Table 3: Full-Sample Connectedness among Currencies, Ten-Days Ahead

	r	v	s
r	83.47	13.16	3.37
v	10.00	89.29	0.71
s	10.63	2.90	86.47

NOTE: The connectedness matrix is computed using normalised generalised forecast error variance decompositions following Diebold and Yilmaz (2014) under the block aggregation routine devised by Greenwood-Nimmo et al. (2015a). All values are measured in percentage points such that each row sums to 100% by construction. The depth of shading reflects the strength of the associated heatwave/spillover effect, with darker shading indicating a stronger effect.

Table 4: Full-Sample Connectedness among Variable Groups, Ten-Days Ahead

		$\overline{F}_t$	$\underline{F}_t$	$\overline{T}_t$	$\underline{T}_t$	$\overline{V}_t$	$\underline{V}_t$
Full Sample	$\overline{S}_t$		32%	6%		13%	
	$\underline{S}_t$	26%			4%		21%
Pre-ZLB Period	$\overline{S}_t$		62%				
	$\underline{S}_t$	35%					
Crisis Period	$\overline{S}_t$			21%		45%	
	$\underline{S}_t$				6%		33%

NOTE: Following the definition in Section 5, $\overline{x}_t$ ($\underline{x}_t$) is a binary variable indicating periods in which the variable $x_t \in \{S_t, F_t, T_t, V_t\}$ records a new high (low) relative to its historical values over a period of 250 trading days. The values reported are pseudo-hit-rates computed following (19). A 'hit' is defined as a new high/low in the spillover index occuring within ±5 trading days of a new high/low in the named macro-financial variable (F_t, T_t or V_t). The full sample is 08-Dec-2000 to 14-Oct-2014 (4,571 trading days), the pre-ZLB sample is 08-Dec-2000 to 31-Dec-2008 (2,077 trading days) and the crisis sample is 15-Sep-2008 to 14-Oct-2014 (1,571 trading days).

Table 5: Pseudo-Hit-Rates over the Full Sample and Selected Subsamples

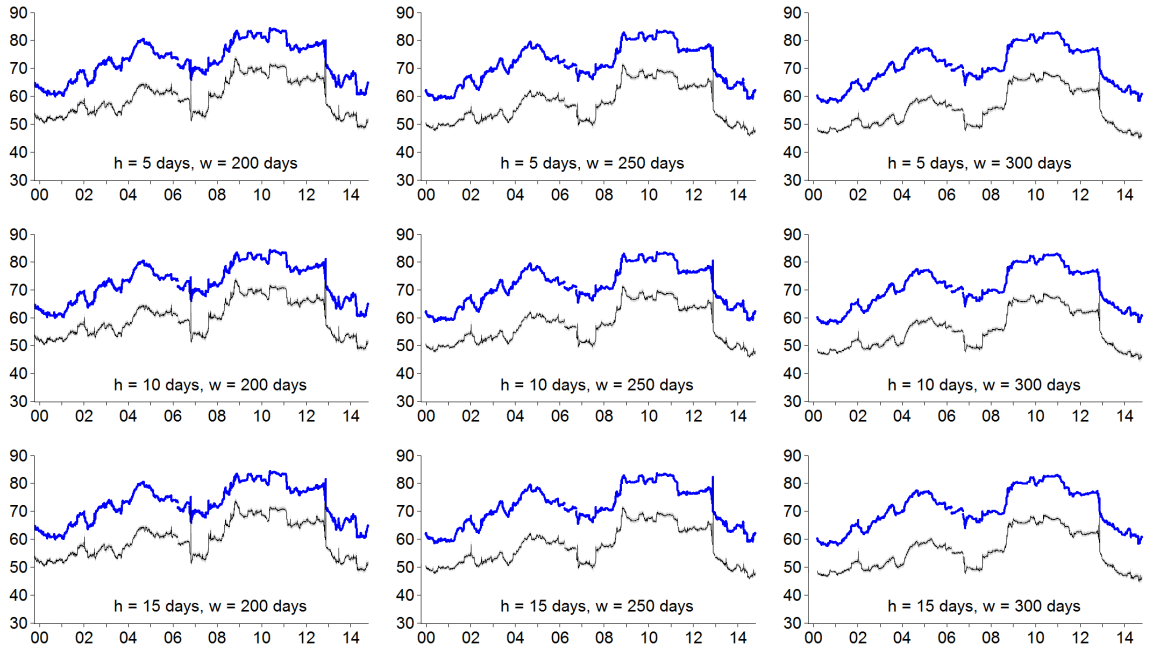

NOTE: We consider windows of $w = (200, 250, 300)$ days, predictive horizons of $h = (5, 10, 15)$ days and a variety of randomly drawn Cholesky orderings. In each panel, the heavy solid line shows the result using order-invariant GVD, the gray band is the $[10\%, 90\%]$ interval based on 1,000 randomly-selected Cholesky orderings and the fine solid line is the mean under the 1,000 Cholesky orderings. In each case, the correlation between our baseline spillover index and the mean of the Cholesky spillover indices is between 0.95 and 0.96.

Figure 1: Sensitivity to the Window Length, Forecast Horizon and the use of Orthogonalisation

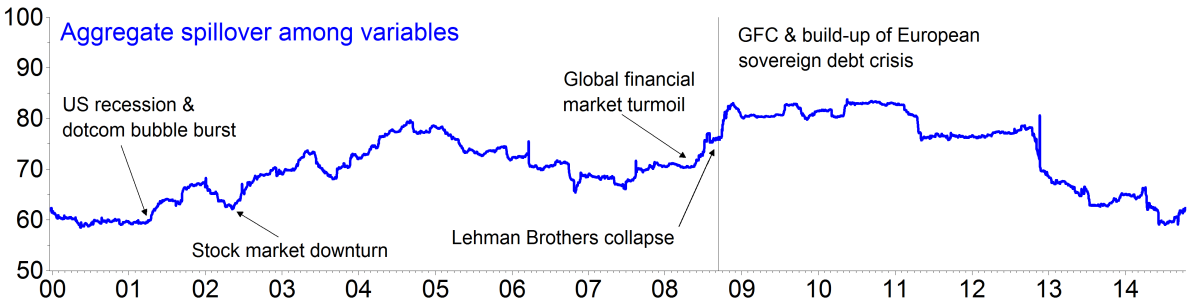

NOTE: Results are obtained from rolling regression of a VAR(1) specification over a rolling window of 250 days at the 10 days ahead forecast horizon. The horizontal time axis records the end date of the rolling samples. The unit of measurement is percent.

Figure 2: Rolling Aggregate Spillover Index, Ten-Days Ahead

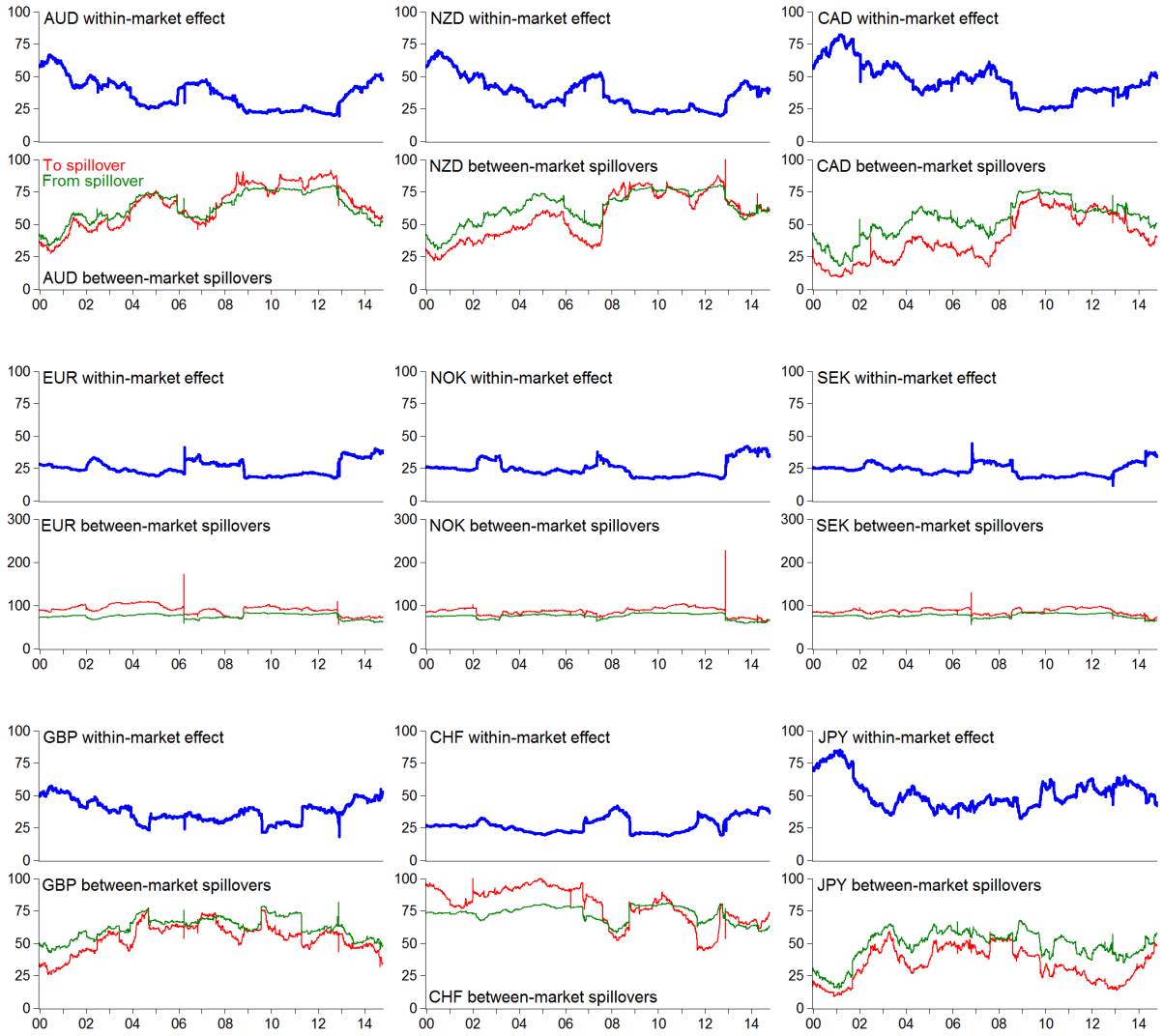

NOTE: Results are obtained from rolling regression of a VAR(1) specification over a rolling window of 250 days at the 10 days ahead forecast horizon. The horizontal time axis records the end date of the rolling samples. The unit of measurement is percent.

Figure 3: Rolling Connectedness among Markets

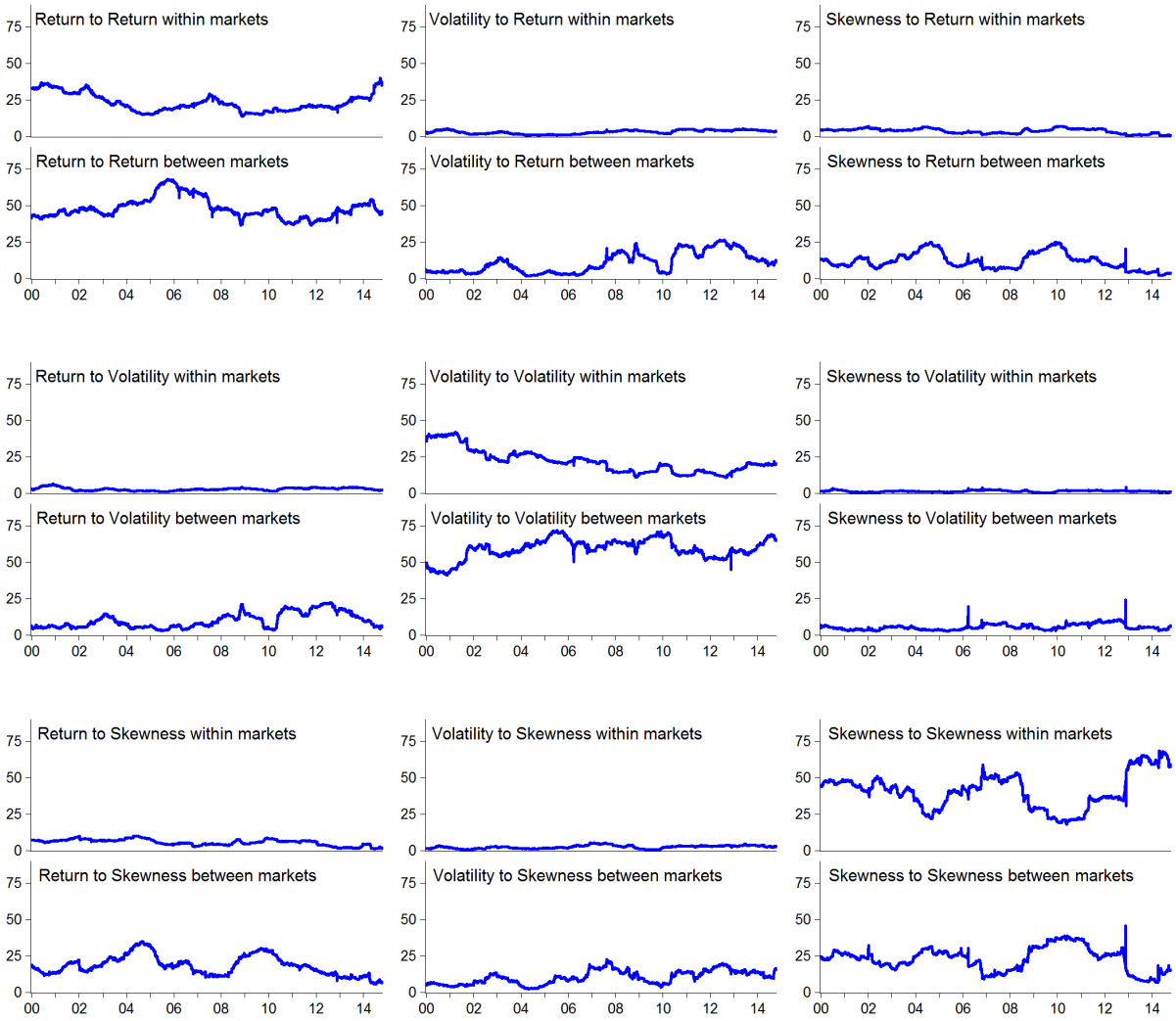

NOTE: Results are obtained from rolling regression of a VAR(1) specification over a rolling window of 250 days at the 10 days ahead forecast horizon. The horizontal time axis records the end date of the rolling samples. The unit of measurement is percent.

Figure 4: Rolling Connectedness among Moments

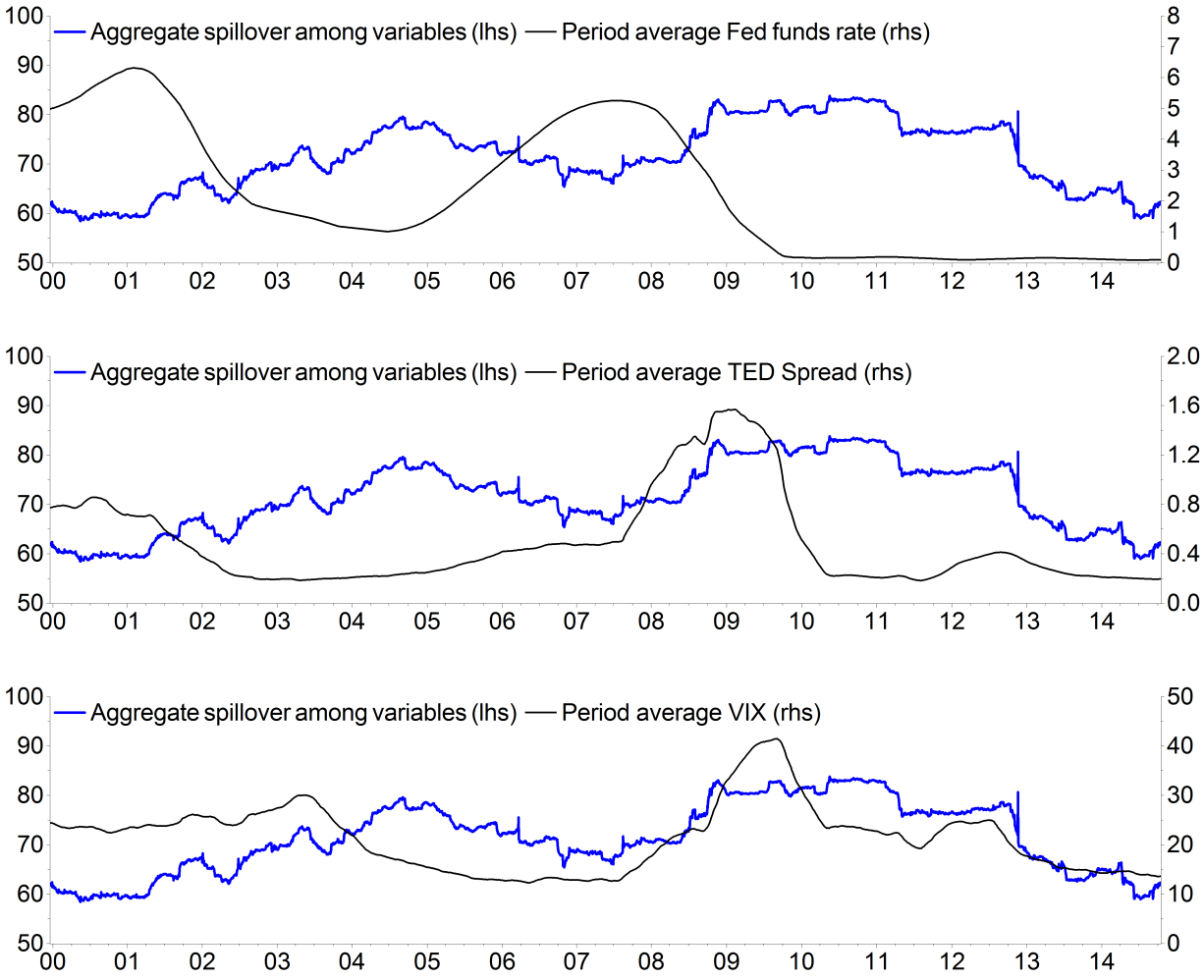

NOTE: The graphs plot the variable-level aggregate spillover index shown in Figure 2 against the period averages of the effective Federal Funds Rate, the TED spread and the VIX, respectively. The period average of the Federal funds rate at time t, for example, is computed as the mean of the effective Federal funds rate over the 250 trading days from $t - 249, \ldots, t$. This matches the data window used to compute the value of spillover index reported at time t. Data for the effective Federal Funds Rate, the TED spread and the VIX were obtained from the Federal Reserve Economic Data Service.

Figure 5: Spillover Index versus Selected Financial Indicators

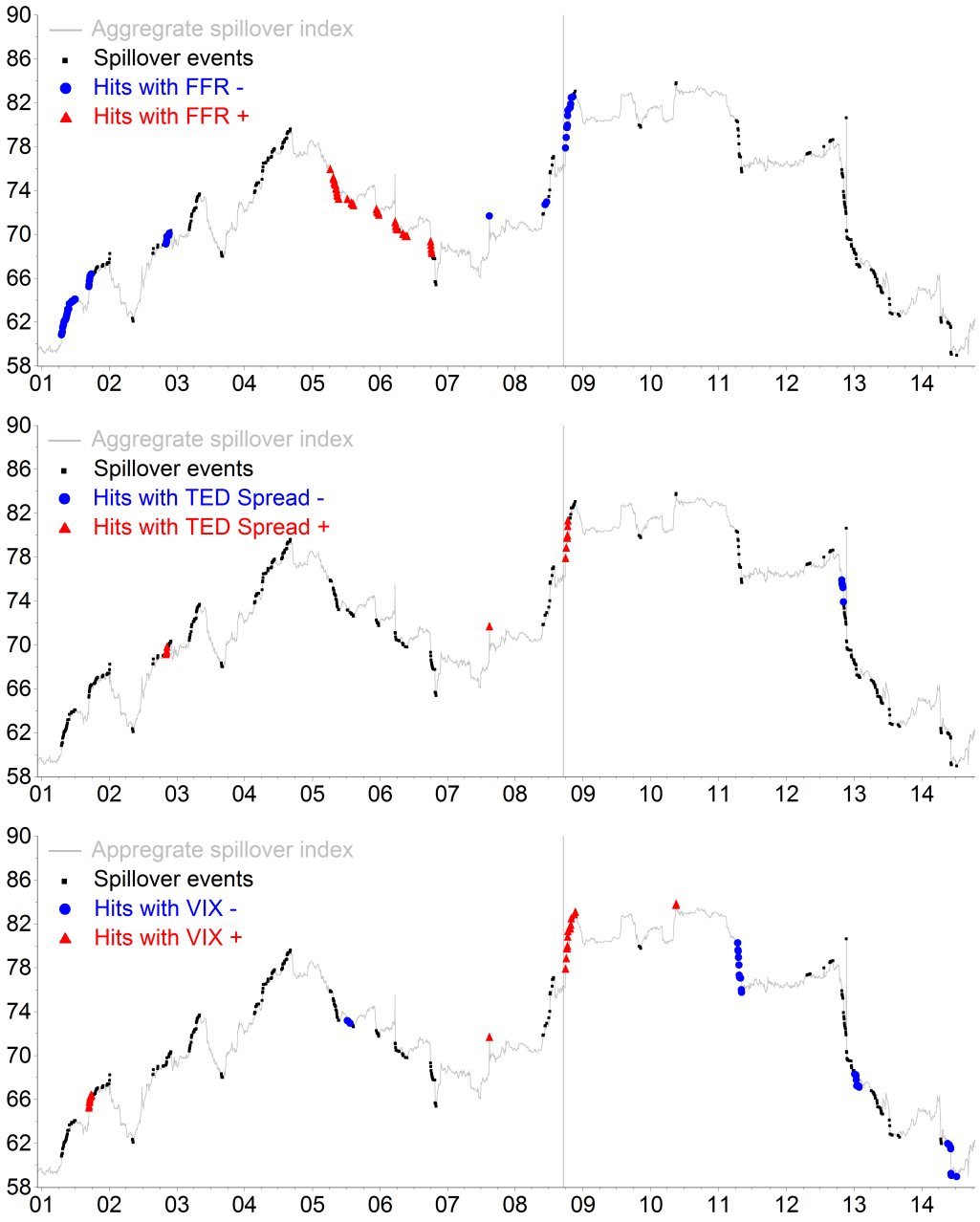

NOTE: The upper panel shows the aggregate spillover among variables first reported in Figure 2 in gray. Each occasion in which the spillover index records a new 250-day high or low value is marked with either a blue dot, a red triangle or a black dot. Each blue dot indicates an occasion where the spillover index reaches a new 250 day high *and* the Federal funds rate reaches a new 250 day low within ±5 trading days. Each red triangle indicates an occasion where the spillover index reaches a new 250 day low *and* the Federal funds rate reaches a new 250 day high within ±5 trading days. Finally, each black dot denotes an occasion where the spillover index records a new 250 day high or low and there is no matching event in the Federal funds rate within ±5 trading days. The middle and lower panels replicate this analysis having replaced the Federal funds rate with the TED spread and the VIX, respectively. The vertical line in each panel corresponds to the collapse of Lehman Brothers. Note that the scale of the vertical axis differs from that used in Figures 2 and 5.

Figure 6: Pseudo-Hit-Rate Analysis showing the Timing of Hits

Appendix A: Computation of the Risk Neutral Moments

FX option conventions

FX options are quoted in terms of their Garman and Kohlhagen (1983) implied volatilities. While the options are quoted in terms of their implied volatilities, the computation of the risk-neutral moments requires the actual prices of the options, since the method used is model-free. Given the implied volatilities, the actual prices of call and put options for currency i can be recovered using the Garman and Kohlhagen (1983) option pricing formulae:

$$C_{i,t}(K_i,\tau) = e^{-r^d_{t,\tau}}\left[F^i_{t,\tau}N(d_1) - K_iN(d_2)\right] \tag{A.1}$$

$$P_{i,t}(K_i,\tau) = e^{-r^d_{t,\tau}}\left[K_iN(-d_2) - F^i_{t,\tau}N(-d_1)\right] \tag{A.2}$$

where

$$d_1 = \frac{\ln\left(\frac{F^i_{t,\tau}}{K_i}\right) + \frac{1}{2}\sigma^2_t(K_i,\tau)\tau}{\sigma_t(K_i,\tau)\sqrt{\tau}}; \quad d_2 = d_1 - \sigma_t(K_i,\tau)\sqrt{\tau} \tag{A.3}$$

and where $C_{i,t}(K_i,\tau)$ and $P_{i,t}(K_i,\tau)$ are the prices of call and put options respectively for currency i, with a strike price of K_i and a maturity of τ (which is expressed as a fraction of a year). Furthermore, $F^i_{t,\tau}$ is the forward rate for currency i with maturity τ, $r^d_{t,\tau}$ is the annualised domestic interest rate (taken to be the U.S. interest rate in this paper) with maturity τ and $N(\cdot)$ is the cumulative distribution function of the normal distribution. Finally, $\sigma_t(K_i,\tau)$ is the volatility of exchange rate changes implied by the option pricing formula. Given an implied volatility quote and the strike price, the price of the option can therefore be easily computed.

In the over the counter market, implied volatility quotes for FX options are generally not given in terms of their strike prices. They are instead given for fixed option deltas. The option deltas are obtained by differentiating the value of the relevant option with respect to the spot exchange rate, $S_{i,t}$. These are given below for call and put options respectively:

$$\delta_c = e^{-r^i_{t,\tau}\tau}N(d_1) \tag{A.4}$$

$$\delta_p = e^{-r^i_{t,\tau}\tau}N(-d_1) \tag{A.5}$$

where $r^i_{t,\tau}$ is the interest rate for currency i with maturity τ. In this paper, we use the no-arbitrage

covered interest rate parity condition given by

$$e^{r^i_{t,\tau}\tau} = e^{r^d_{t,\tau}\tau}\frac{S_{i,t}}{F^i_{t,\tau}} \tag{A.6}$$

to determine $r^i_{t,\tau}$.

Option market makers generally quote implied volatilities for portfolios of out of the money (OTM) 25δ and 10δ options contracts (e.g. quotes for risk reversals and butterfly strangles) as well as an at the money (ATM) delta-neutral (0δ) straddle. From these, one can get implied volatility quotes for options at five different strike prices: 25δ put and call options, 10δ put and call options and ATM put and call options. With fixed deltas and implied volatility quotes, the strike prices can be backed out from the Garman and Kohlhagen (1983) formulae. The put and call strike prices with deltas of δ_c and δ_p are given by:

$$K_{i,\delta_c} = F^i_{t,\tau}\exp\left(\frac{1}{2}\sigma^2_t(\delta_c,\tau)\tau - \sigma_t(\delta_c,\tau)\sqrt{\tau}N^{-1}\left[e^{r^i_{t,\tau}\tau}\delta_c\right]\right) \tag{A.7}$$

$$K_{i,\delta_c} = F^i_{t,\tau}\exp\left(\frac{1}{2}\sigma^2_t(\delta_c,\tau)\tau + \sigma_t(\delta_c,\tau)\sqrt{\tau}N^{-1}\left[-e^{r^i_{t,\tau}\tau}\delta_c\right]\right) \tag{A.8}$$

where $N^{-1}(\cdot)$ is the inverse of the cumulative distribution function for the normal distribution.

Finally, we can set $\delta_{c,ATM} + \delta_{p,ATM} = 0$ and solve to get the ATM strike price for the delta-neutral straddle, which is given by:

$$\begin{aligned} K_{i,ATM} &= S_{i,t}e^{r^d_{t,\tau} - r^i_{t,\tau}\tau + \frac{1}{2}\sigma^2_t(ATM,\tau)\tau} \\ &= F^i_{t,\tau}e^{\frac{1}{2}\sigma^2_t(ATM,\tau)\tau} \end{aligned} \tag{A.9}$$

Computing risk-neutral moments from FX options prices

Breedon and Litzenberger (1978) were the first to show that a complete set of options on an asset allow the asset's entire risk-neutral distribution to be recovered from the option prices. If we consider an arbitrary state-contigent payoff for currency i at time $t+\tau$, that depends on the future

spot rate, and denote it by $H(S_{i,t+\tau})$, it can be valued by

$$\begin{aligned} p_{i,t} &= \exp(-r^d_{t,\tau}) \int_0^\infty H(S_{i,t+\tau}) q(S_{i,t+\tau}) dS_{i,t+\tau} \\ &= \exp(-r^d_{t,\tau}) E^Q_t(H(S_{i,t+\tau})) \end{aligned} \tag{A.10}$$

where $q(S_{i,t+\tau})$ is the density of the risk-neutral distribution and $E^Q_t(\cdot)$ is the expectation under the risk neutral measure Q.

In practice, we don't have a complete set of options. However, Bakshi and Madan (2000) show that any payoff with bounded expectation under the risk neutral distribution can be spanned by a continuum of out of the money put and call options. This allows the state-contingent payoff $H(S_{i,t+\tau})$ to be priced by

$$\begin{aligned} p_{i,t} &= \exp(-r^d_{t,\tau})(H(\bar{S}_i) - \bar{S}_i) + H_{SS}(\bar{S}_i) S_{i,t} \\ &+ \int_0^{\bar{S}_i} H_{SS}(K_i) P_t(K_i, \tau) dK_i + \int_{\bar{S}_i}^\infty H_{SS}(K_i) C_t(K_i, \tau) dK_i \end{aligned} \tag{A.11}$$

where K_i are option strike prices, H_S and H_{SS} are the first and second derivative of the state contingent payoff function and $C_t(K_i, \tau)$ and $P_t(K_i, \tau)$ are the prices of call and put options with a strike price of K_i. $\bar{S}_i$ is a future value of the spot exchange rate for currency i, typically taken to be equal to the forward rate $F^i_{t,\tau}$.

Bakshi et al. (2003) show that if we set $H(S_{t+\tau}) = (\Delta \ln(S_{t+\tau}))^n$, the values of the discounted non-central moments of the risk-neutral distribution can be valued by (A.11). The discounted risk-neutral volatility, risk-neutral skewness and risk-neutral kurtosis of exchange rate changes for currency i are denoted by $V_{i,t}(\tau)$, $W_{i,t}(\tau)$ and $X_{i,t}(\tau)$ respectively and are given by

$$\begin{aligned} V_{i,t}(\tau) &= \int_{\bar{S}_i}^\infty \frac{2\left(1 - \ln\left(\frac{K_i}{\bar{S}_i}\right)\right)}{K_i^2} C_{i,t}(K_i, \tau) dK_i \\ &+ \int_0^{\bar{S}_i} \frac{2\left(1 + \ln\left(\frac{\bar{S}_i}{K_i}\right)\right)}{K_i^2} P_{i,t}(K_i, \tau) dK_i \end{aligned} \tag{A.12}$$

$$W_{i,t}(\tau) = \int_{\bar{S}_i}^{\infty} \frac{6\ln\left(\frac{K_i}{\bar{S}_i}\right) - 3\left(\ln\left(\frac{K_i}{\bar{S}_i}\right)\right)^2}{K_i^2} C_{i,t}(K_i,\tau)dK_i + \int_0^{\bar{S}_i} \frac{6\ln\left(\frac{\bar{S}_i}{K_i}\right) + 3\left(\ln\left(\frac{\bar{S}_i}{K_i}\right)\right)^2}{K_i^2} P_{i,t}(K_i,\tau)dK_i \tag{A.13}$$

$$X_{i,t}(\tau) = \int_{\bar{S}_i}^{\infty} \frac{12\left(\ln\left(\frac{K_i}{\bar{S}_i}\right)\right)^2 - 4\left(\ln\left(\frac{K_i}{\bar{S}_i}\right)\right)^3}{K_i^2} C_{i,t}(K_i,\tau)dK_i + \int_0^{\bar{S}_i} \frac{12\left(\ln\left(\frac{\bar{S}_i}{K_i}\right)\right)^2 + 4\left(\ln\left(\frac{\bar{S}_i}{K_i}\right)\right)^3}{K_i^2} P_{i,t}(K_i,\tau)dK_i \tag{A.14}$$

Using these and doing some transformations gives the risk-neutral volatility, risk neutral skewness and risk neutral kurtosis, which are given by

$$\text{VOL}_{i,t}^{RN}(\tau) = \left[e^{r_{t,\tau}^d \tau} V_{i,t}(\tau) - \mu_{i,t}(\tau)^2\right]^{\frac{1}{2}} \tag{A.15}$$

$$\text{SKEW}_{i,t}^{RN}(\tau) = \frac{e^{r_{t,\tau}^d \tau} W_{i,t}(\tau) - 3\mu_{i,t}(\tau) e^{r_{t,\tau}^d \tau} V_{i,t}(\tau) + 2\mu_{i,t}(\tau)^3}{\left[e^{r_{t,\tau}^d \tau} V_{i,t}(\tau) - \mu_{i,t}(\tau)^2\right]^{\frac{3}{2}}} \tag{A.16}$$

$$\text{KURT}_{i,t}^{RN}(\tau) = \frac{e^{r_{t,\tau}^d \tau} X_{i,t}(\tau) - 4\mu_{i,t}(\tau) e^{r_{t,\tau}^d \tau} W_{i,t}(\tau) + 6\mu_{i,t}(\tau)^2 e^{r_{t,\tau}^d \tau} V_{i,t}(\tau) - 3\mu_{i,t}(\tau)^4}{\left[e^{r_{t,\tau}^d \tau} V_{i,t}(\tau) - \mu_{i,t}(\tau)^2\right]^2} \tag{A.17}$$

where the mean of the risk neutral distribution is given by

$$\mu_{i,t}(\tau) = e^{(r_{t,\tau}^d - r_{t,\tau}^i)\tau} - 1 - e^{r_{t,\tau}^d \tau}\left(\frac{V_{i,t}(\tau)}{2} + \frac{W_{i,t}(\tau)}{6} + \frac{X_{i,t}(\tau)}{24}\right) \tag{A.18}$$

To compute these risk neutral moments requires a continuum of out of the money call and put options. In practice though, there is only a limited range of strikes at which options are quoted. However, Jiang and Tian (2005) argue based on sensitivity results that the available cross section of foreign exchange options is sufficient, when combined with interpolation to ensure the errors in extracting the risk neutral moments are very small. To interpolate the implied volatility function, we use the vanna-volga method (see Castagna and Mercurio, 2007). In addition, we extrapolate the implied volatility functions by appending flat tails.

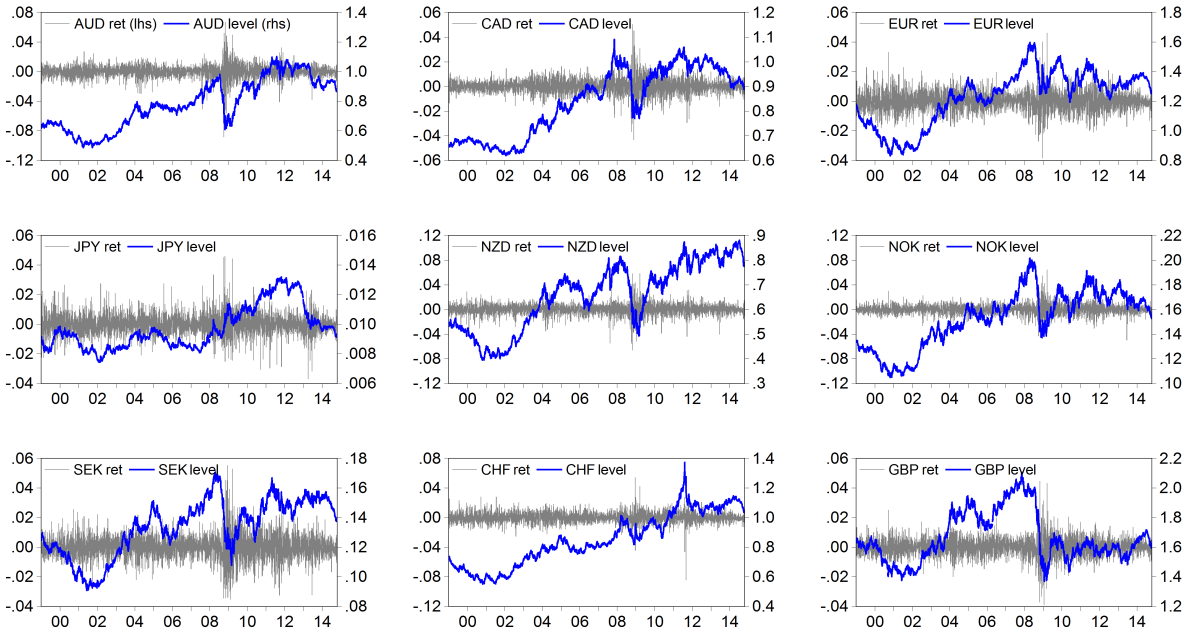

Figure A.1: Spot Exchange Rates and Daily Log Returns by Market

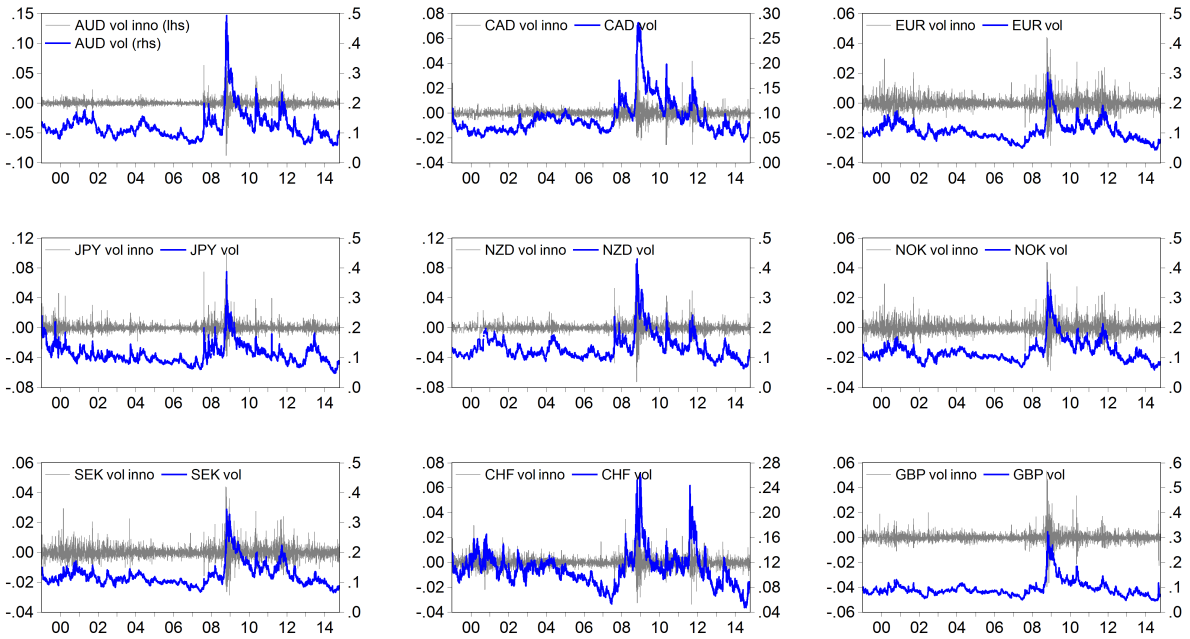

Note: The RNV innovations are computed as the residuals from an AR(1) process following the approach adopted by Menkhoff et al. (2012).

Figure A.2: Level and Innovations of Risk-Neutral Volatility (RNV) by Market

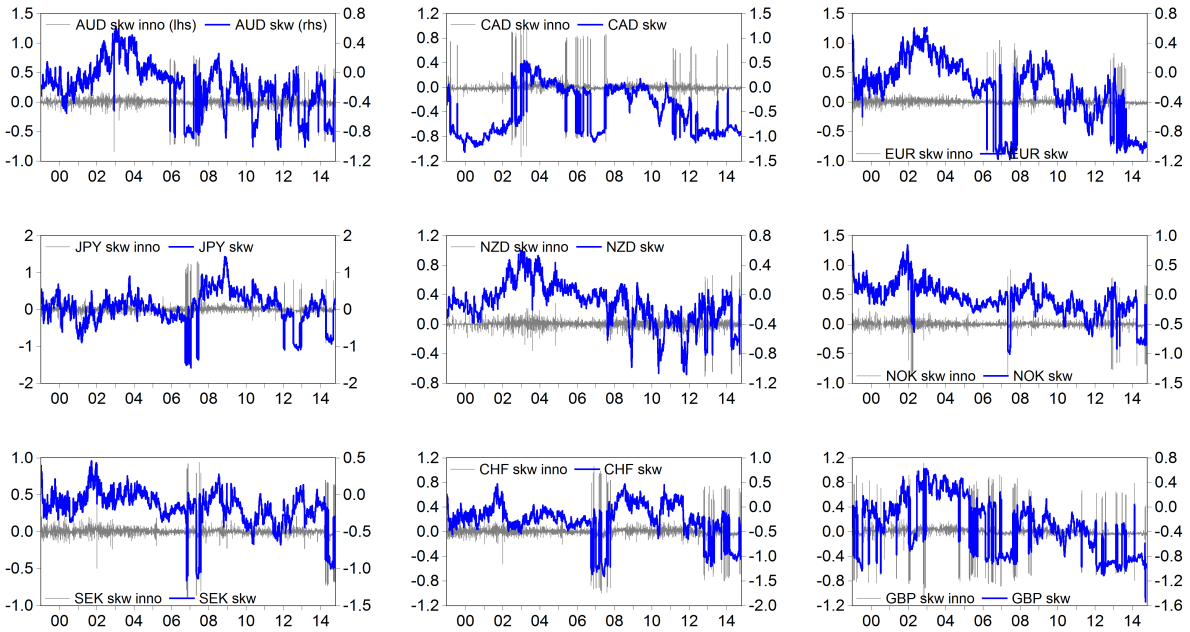

NOTE: The RNS innovations are computed as the residuals from an AR(1) process following the approach adopted by Chang et al. (2013).

Figure A.3: Level and Innovations of Risk-Neutral Skewness (RNS) by Market

Appendix B: Aggregation into Variable Groups

To evaluate the connectedness among the three variables r, v and s for all N markets collectively, one simply reorders the variables in the VAR to obtain $\mathbf{y}_t = (\mathbf{r}_t, \mathbf{v}_t, \mathbf{s}_t)'$ where $\mathbf{r}_t = (r_{1,t}, r_{2,t}, \ldots, r_{N,t})$, $\mathbf{v}_t = (v_{1,t}, v_{2,t}, \ldots, v_{N,t})$ and $\mathbf{s}_t = (s_{1,t}, s_{2,t}, \ldots, s_{N,t})$. In this case, we may write the h-step ahead connectedness matrix as follows:

$$\mathbb{C}^{(h)} = \begin{bmatrix} \mathbf{B}^{(h)}_{r\leftarrow r} & \mathbf{B}^{(h)}_{r\leftarrow v} & \mathbf{B}^{(h)}_{r\leftarrow s} \\ \mathbf{B}^{(h)}_{v\leftarrow r} & \mathbf{B}^{(h)}_{v\leftarrow v} & \mathbf{B}^{(h)}_{v\leftarrow s} \\ \mathbf{B}^{(h)}_{s\leftarrow r} & \mathbf{B}^{(h)}_{s\leftarrow v} & \mathbf{B}^{(h)}_{s\leftarrow s} \end{bmatrix} \tag{B.1}$$

where we aggregate into $g = 3$ groups each composed of $m = N$ variables:

$$\mathbf{B}^{(h)}_{r\leftarrow r} = \begin{bmatrix} \theta^{(h)}_{r_1\leftarrow r_1} & \theta^{(h)}_{r_1\leftarrow r_2} & \cdots & \theta^{(h)}_{r_1\leftarrow r_N} \\ \theta^{(h)}_{r_2\leftarrow r_1} & \theta^{(h)}_{r_2\leftarrow r_2} & \cdots & \theta^{(h)}_{r_2\leftarrow r_N} \\ \vdots & \vdots & \ddots & \vdots \\ \theta^{(h)}_{r_N\leftarrow r_1} & \theta^{(h)}_{r_N\leftarrow r_2} & \cdots & \theta^{(h)}_{r_N\leftarrow r_N} \end{bmatrix}, \quad \mathbf{B}^{(h)}_{r\leftarrow v} = \begin{bmatrix} \theta^{(h)}_{r_1\leftarrow v_1} & \theta^{(h)}_{r_1\leftarrow v_2} & \cdots & \theta^{(h)}_{r_1\leftarrow v_N} \\ \theta^{(h)}_{r_2\leftarrow v_1} & \theta^{(h)}_{r_2\leftarrow v_2} & \cdots & \theta^{(h)}_{r_2\leftarrow v_N} \\ \vdots & \vdots & \ddots & \vdots \\ \theta^{(h)}_{r_N\leftarrow v_1} & \theta^{(h)}_{r_N\leftarrow v_2} & \cdots & \theta^{(h)}_{r_N\leftarrow v_N} \end{bmatrix}$$

and likewise for the remaining blocks. Block connectedness measures can be computed at the level of the three variable groups based on (B.1) exactly as described in Section 2 of the main text.

Appendix C: Robustness to the Inclusion of Risk-Neutral Kurtosis

To verify that the exclusion of the risk-neutral kurtosis (RNK) from the model does not materially affect our results, we re-estimated the system including realised returns, RNV, RNS and RNK for the same group of markets over the same sample period. We then repeated our analysis and found that the results under each setting were qualitatively similar. An illustration of this similarity is provided in Figure C.1 below, which recreates Figure 2 from the main text for the cases with and without kurtosis.

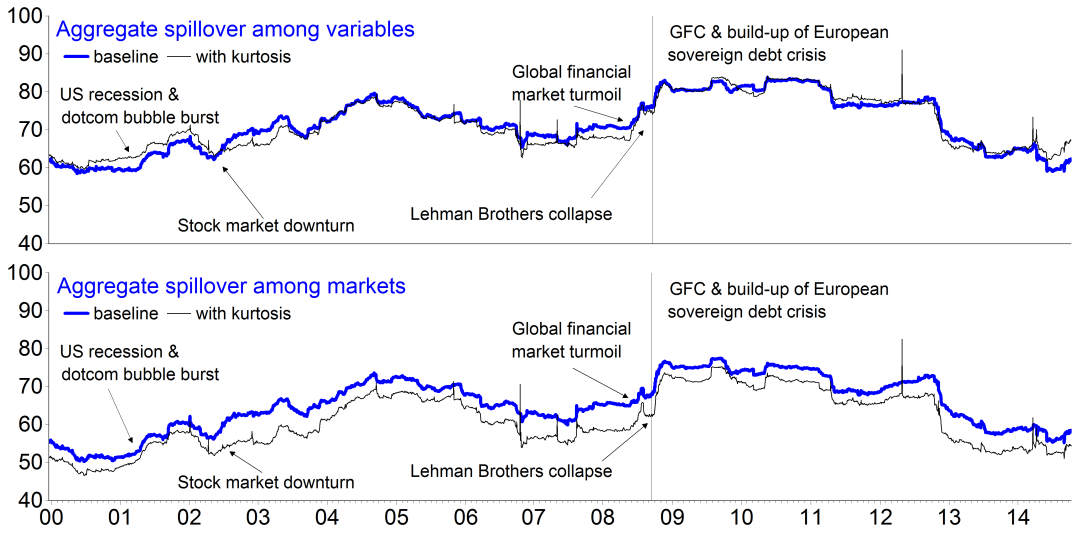

NOTE: In each panel, the heavy line corresponds to our baseline result (excluding RNK) while the fine line corresponds to the result from a system including RNK.

Figure C.1: Robustness of Spillovers, with and without Kurtosis

Table C.1 shows that the spillover indices with and without kurtosis comove closely, so the inclusion of kurtosis within the system does not yield much additional information.

	Spillover among variables	Spillover among markets
Correlation Coefficient	0.96	0.98
Directional Accuracy	0.76	0.78

NOTE: The directional accuracy measure records the proportion of periods in which our baseline spillover index moves in the same direction as the alternative version including kurtosis.

Table C.1: Comovement of Spillover Indices, with and without Kurtosis